Online Appendix

Non-linearities, sticky prices and the transmission mechanism of monetary policy

Guido Ascari*
University of Oxford
University of Pavia
RCEA

Timo Haber†
University of Cambridge

Contents

A Introduction **3**

B Estimation technique **3**

C Robustness: Size dependent impulse response **6**

C.1 Recursive estimates 7

C.2 Alternative specification with quadratic and cubic terms 7

C.3 Unscaled impulse responses to large and small shocks 9

D Robustness: Smooth Transition Local Projection **10**

D.1 Varying the regime switching parameter 10

D.2 Varying the percentile of inflation parameter 10

D.3 Using HP-Filtered PCE Inflation 10

D.4 Using the trend inflation measure from Ireland (2007) 11

*Address: Department of Economics, University of Oxford, Manor Road, Oxford OX1 3UQ, United Kingdom. E-mail address: guido.ascari@economics.ox.ac.uk.

†Address: Faculty of Economics, University of Cambridge, Austin Robinson Building, Sidgwick Avenue, Cambridge CB3 9DD, United Kingdom. E-mail address: tfh27@cam.ac.uk.

E Robustness: Both tests **11**

E.1 Alternative price measure: CPI 11

E.2 Controlling for commodity prices 11

E.3 Controlling for financial frictions 12

E.4 Non-linear Romer and Romer (2004) regression 12

E.5 Shocks from a smooth transition VAR 13

E.6 Including leads and lags of the shocks 14

E.7 Quarterly estimation using GDP as output measure 14

E.8 Quarterly estimation including fiscal policy controls 15

E.9 Unsmoothed results 15

F Shock distribution: Asymmetries and business-cycle dependencies **15**

G Hansen (1992) test procedure **17**

H Figures **21**

I Tables **58**

A Introduction

In this appendix we describe the estimation technique, perform a thorough sensitivity analysis for our results in the main text of the paper and describe further details of the Hansen (1992) test. First, we describe the estimation technique of smooth local projections by Barnichon and Brownlees (2019) in section B. Second, we present further robustness checks specific to our test of the size effect of monetary shocks (equation (1) in the main text) in section C. Third, we present robustness checks specific to our test of regime dependency of monetary shocks (equation (2) in the main text) in section D. Fourth, we present a number of robustness checks on the results regarding both tests in section E. We also provide some additional figures displaying the shock distribution and results regarding their regime dependency in section F. Finally, we discuss our application of the Hansen (1992) coefficient constancy test in more detail in section G. All the figures are collected in section H and all the tables are collected in section I. The numbers of equations and sections purely in Arabic, with no letters, refer to the equations and the sections in the main text of the paper.

B Estimation technique

In this section we describe the methodology used for our estimation. We follow Barnichon and Brownlees (2019) very closely and advise the reader to consult their work in case some aspects remain unclear.

Smooth local projections. Below we will set out the estimation technique, using the local projection (1) as our reference point. Note, however, that the same technique applies to all other local projections too, including (2) and the two coefficients of interest β_h^{HI} and β_h^{LO}.

Recall our main equation for the first test (1), repeated below for convenience:

$$y_{t+h} = \alpha_h + \tau_h t + \beta_h e_t + \zeta_h (e_t \cdot |e_t|) + \sum_{k=1}^{K} \gamma_{h,k} w_{t,k} + v_{t+h}, \tag{B1}$$

We can approximate both the β_h and the ζ_h coefficient using B-spline basis function expansions as follows:

$$\beta_h \approx \sum_{j=1}^{J} b_j B_j(h) \tag{B2}$$

$$\zeta_h \approx \sum_{j=1}^{J} z_j B_j(h) \tag{B3}$$

where $B_j : \mathbb{R} \to \mathbb{R}$ for $j = 1, \ldots, J$ is a set of B-spline basis function and b_j and z_j for $j = 1, \ldots, J$ are a set of scalar parameters. With this we can write (B1) as:

$$y_{t+h} = \alpha_h + \tau_h t + \sum_{j=1}^{J} b_j B_j(h) e_t + \sum_{j=1}^{J} z_j B_j(h)(e_t \cdot |e_t|) + \sum_{k=1}^{K} \gamma_{h,k} w_{t,k} + v_{t+h}, \tag{B4}$$

One can represent this in linear regression form. Let $\mathcal{Y}_t$ for $t = 1, \ldots, T$ be defined as the vector $(y_{\min(t,T-H)}, \ldots, y_{\min(T,t+H)})'$ with size H. Let $\mathcal{X}_{\beta,t}$ and $\mathcal{X}_{\zeta,t}$ be defined as $H \times J$ matrices where the (h, j)th element is $B_j(h)e_t$ and $B_j(h)(e_t \cdot |e_t|)$, respectively. Define $\mathcal{X}_{\alpha,t}$ as a diagonal $H \times H$ matrix with 1s on its main diagonal. Define $\mathcal{X}_{\tau,t}$ also as a diagonal $H \times H$ matrix with t on its main diagonal. Define $\mathcal{X}_{\gamma,t}$ also as a diagonal $H \times H$ matrix with $w_{t,k}$ on its main diagonal for $k = 1, \ldots, K$. Stacking these horizontally we obtain $\mathcal{X}_t = (\mathcal{X}_{\alpha,t}, \mathcal{X}_{\tau,t}, \mathcal{X}_{\beta,t}, \mathcal{X}_{\zeta,t}, \mathcal{X}_{\gamma,t})$. We can now write equation (B4) as

$$\mathcal{Y}_t = \mathcal{X}_t \theta + \mathcal{U}_t \tag{B5}$$

where $\mathcal{U}_t$ denotes the $H \times 1$ prediction error vector term. Finally, one can stack these for $t = 1, \ldots, T$ to obtain $\mathcal{Y}, \mathcal{X}$ and $\mathcal{U}$. The smooth local projections can then be estimated

by generalized ridge estimation:

$$\hat{\theta} = \arg\min_{\theta}\{||\mathcal{Y} - \mathcal{X}\theta||^2 + \lambda\theta'\mathbf{P}\theta\} \tag{B6}$$

$$= (\mathcal{X}'\mathcal{X} + \lambda\mathbf{P})^{-1}\mathcal{X}'\mathcal{Y}, \tag{B7}$$

where λ is a positive shrinkage parameter and $\mathbf{P}$ is a symmetric positive semidefinite penalty matrix. The value of λ determines the bias/variance trade-off in the estimation. The estimation collapses to least squares estimator when $\lambda = 0$ whilst the estimator is biased with a large value of λ but may have a smaller variance.

Penalty matrix. We use a penalty matrix $\mathbf{P} = \mathbf{D}_r'\mathbf{D}_r$ where $\mathbf{D}_r'$ is the matrix representation of Δ^r, the r-th difference operator. This lets the estimated impulse response - with a very large λ - shrink to the $r-1$ polynomial. We set $r = 3$ so that the limit polynomial is quadratic.

Shrinkage parameter We select the optimal λ using k-fold cross validation (Racine, 1997). We set $k = 0$ so that the cross validation function becomes:

$$CV = \frac{1}{T}\sum_{t=1}^{T}\frac{\hat{\mathcal{U}}_t^2}{(1-h_{tt})^2} \tag{B8}$$

where h_{tt} denotes the tth diagonal element of the projection matrix $\mathcal{X}_t(\mathcal{X}_t'\mathcal{X}_t + \lambda\mathbf{P})^{-1}\mathcal{X}_t'$.

Inference We also follow Barnichon and Brownlees (2019) in conducting inference. We estimate the Newey and West (1987) variance of $\hat{\theta}$ as follows:

$$\begin{aligned}\widehat{\mathbf{V}}(\hat{\theta}) =& T\left[\sum_{t=1}^{T}\mathcal{X}_t'\mathcal{X}_t + \lambda\mathbf{P}\right]^{-1}\left[\hat{\mathbf{\Gamma}}_0 + \sum_{l=1}^{L} w_l\left(\hat{\mathbf{\Gamma}}_l + \hat{\mathbf{\Gamma}}_l'\right)\right] \\ &\times\left[\sum_{t=1}^{T}\mathcal{X}_t'\mathcal{X}_t + \lambda\mathbf{P}\right]^{-1}\end{aligned} \tag{B9}$$

where $w_l = 1 - l/(1+L)$ and $\hat{\mathbf{\Gamma}}_l = \frac{1}{T}\sum_{t=l+1}^{T}\mathcal{X}_t'\hat{\mathcal{U}}_t\hat{\mathcal{U}}_{t-l}'\,\mathcal{X}_{t-l}$ with $\hat{\mathcal{U}}_t$ denoting regression residuals. We set L to H and λ to 0.5 times the degree of shrinkage determined by k -fold

cross-validation. We construct the standard errors for coefficient β_h as $\sqrt{\mathbf{B}(h)'\widehat{\mathbf{V}}(\hat{b})\mathbf{B}(h)}$ where $\mathbf{B}(h) = (B_1(h), \ldots, B_J(h))'$, and $\hat{b}$ and $\widehat{\mathbf{V}}(\hat{b})$ denote the subvector and submatrix of, respectively, $\hat{\theta}$ and $\widehat{\mathbf{V}}(\hat{\theta})$ relative to the b parameter.

Consequently, the $1-p$ confidence interval for β_h is $\mathbf{B}(h)'\hat{b} \pm z_{1-p/2}\sqrt{\mathbf{B}(h)'\widehat{\mathbf{V}}(\hat{b})\mathbf{B}(h)}$, where $z_{1-p/2}$ denotes the $1-p/2$ quantile of a standard normal. And the t-statistic can be computed as $\frac{\beta_h}{\sqrt{\mathbf{B}(h)'\widehat{\mathbf{V}}(\hat{b})\mathbf{B}(h)}}$. An identical procedure applies to the coefficient ζ_h.

Delta method. When constructing functions $g(\hat{\theta})$ that depend on our estimated coefficients we use the Delta method to conduct inference. The variance of these functions can be approximated as:

$$\hat{V}(g(\hat{\theta})) \approx \nabla g(\hat{\theta})'\widehat{\mathbf{V}}(\hat{\theta})\nabla g(\hat{\theta}) \tag{B10}$$

where $\nabla g(\hat{\theta})$ is the Jacobian matrix of $g(\hat{\theta})$ with respect to $\hat{\theta}$.

Non-smoothed and cumulative responses. When estimating non-smoothed responses we set $\lambda = 0$ to obtain the least squares estimates. We also construct cumulative responses from this, by cumulating the non-smoothed response over its projection horizon. The variance matrix for the cumulative estimates can then be obtained with the Delta method, as set out above.

C Robustness: Size dependent impulse response

In this section we perform a number of robustness checks with respect to equation (1), the test for a size-dependent impulse response. In C.1 we conduct a visual stability assessment of recursive estimates of the absolute value interaction term. In C.2 we include the squared and cubed value of the shock instead of the absolute value interaction term. In C.3 we show the impulse responses to a 25bp and a 200bp shock.

C.1 Recursive estimates

We check the stability of the absolute value interaction coefficients by recursively estimating equation (1), adding one month for every new estimation. We start with a third of our sample, corresponding to the 140 months between January 1969 to August 1980. Figures H1, H2 and H3 plot the results for the absolute value interaction term coefficient with respect to PCE inflation, industrial output and the federal funds rate, respectively. The x-axis indicates the horizon of the impulse response, the y-axis indicates the last period in the sample for the recursive estimates and the z-axis indicates the coefficient size. The recursive coefficient sequences are relatively stable. Take, for example, the inflation coefficients with respect to the absolute value interaction of the monetary shock. Qualitatively, the negative and then positive dynamics of this coefficient are certainly constant over the recursive estimation. Furthermore, its size is also relatively similar across different samples, apart from some fluctuations for the long horizons at the beginning of the sample until the mid 1980s.

C.2 Alternative specification with quadratic and cubic terms

Here we consider a different specification for the non-linear local projection to investigate non-linearities in the impulse response function with respect to the size of the shock:

$$y_{t+h} = \alpha_h + \tau_h t + \beta_h e_t + \vartheta_h e_t^2 + \psi_h e_t^3 + \sum_{k=1}^{K} \gamma_{h,k} w_{t,k} + v_{t+h}. \tag{C11}$$

The inclusion of a squared and a cubed shock value accounts for non-linearities in the impulse response function in a different way. The coefficient with respect to squared shocks, ϑ_h, captures possible asymmetries of the impulse response functions with respect to positive and negative shocks. In general, a ϑ_h with a sign equal to that of β_h amplifies the linear coefficient of the impulse response with respect to positive shocks. Conversely, a ϑ_h with an opposite sign to β_h counteracts the linear coefficient of the impulse response

with respect to positive shocks.

The coefficient with respect to cubed shocks, ψ_h, captures possible non-linearities with respect to the size of the shock, and is the main coefficient of interest in this specification. In general, a ψ_h with a sign equal to the one of β_h amplifies the latter coefficient after larger shocks. On the contrary, a ψ_h with an opposite sign to the one of β_h counteracts the latter coefficient after larger shocks. We prefer our benchmark specification (1) to (C11) because a larger shock affects the shape of the impulse response also via the squared term and may thus obfuscate interpretation for our test. Hence, the interaction term in (1) should capture and illustrate the size effect more neatly than the cubed shock term in (C11).

The estimated coefficients are reported in Figure H4. As previously, the three rows correspond to the three response variables, annualized PCE inflation (row 1), industrial production (row 2) and the federal funds rate (row 3). The first column combines all three coefficients of the non-linear impulse response, $\hat{\beta}_h$ (black, solid line), $\hat{\vartheta}_h$ (red, dashed line) and $\hat{\psi}_h$ (green, dashed-dotted line) into one graph. The second column shows the coefficient with respect to the squared shock value ($\hat{\vartheta}_h$) again, together with its 90% confidence interval. The third column depicts the coefficient with respect to the cubed shock value ($\hat{\psi}_h$) again, together with its 90% confidence interval. A similar pattern compared to the main results of Section 4.1 emerges. The literature standard conclusions with respect to the linear coefficients still hold, and, more importantly, also this specification provides a consistent picture with respect to the non-linear interaction terms. The cubed shock coefficient counteracts the linear term for both inflation and output. Larger monetary policy shocks prompt a weaker price and output puzzle at early horizons, and thus a negative overall effect for sufficiently large shocks. Furthermore, there seems to be less persistence as the cubed shock coefficients become significantly positive whilst the linear effect is negative for both inflation and output in the second part of the IRFs. Consequently, this again seems to point towards state-dependency as,

for large shocks, inflation reacts stronger at short horizons and weaker at long horizons. To conclude, results are in line with the main specification of Section 4.1 and confirm our first theoretical predictions once again.

Regarding the squared shock coefficient, there is some weak, statistically insignificant, evidence that prices react more negatively at short horizons for positive (contractionary) monetary policy shocks, reducing somewhat the linear price puzzle. Conversely, negative (expansionary) shocks would prompt an amplified price puzzle. There is stronger and statistically significant evidence that positive shocks reduce the persistence and depth of the inflation impulse response at longer horizons. The squared shock coefficient in the output impulse response is largely insignificant, except for the early horizons where we can also observe a weakening of the output puzzle for positive shocks. This result is consistent with the findings of Cover (1992) or Barnichon and Matthes (2018) that positive money-supply (expansionary) shocks have a weaker effect on output than negative money-supply (contractionary) shocks. However, the coefficient with respect to the federal funds rate is positively significant at the very early horizons, suggesting that monetary policy reacts stronger after positive shocks. Yet, this effect is marginal and dies away quite quickly. Overall, the results suggest asymmetric responses to monetary policy shocks, in accordance with the previous literature on this issue, as the ones in Tenreyro and Thwaites (2016) or Barnichon and Matthes (2018).

C.3 Unscaled impulse responses to large and small shocks

Figure H5 depicts the unscaled (i.e., non-standardised) impulse responses for a 25 basis point shock and a 200 basis point shock and their 90% confidence interval calculated with the Delta method, respectively. This complements Figure 2 in the main text. First, the larger the shock, the quicker inflation decreases. Second, for a large enough shock, the initial price puzzle on impact disappears: the IRF to a large shock is firstly not significantly different from zero and then significantly negative, while it is positive for

some months for small shocks (even if only marginally significantly). Consequently, a sufficiently large shock counteracts the small linear coefficient and switches the sign of the overall impulse response of inflation, removing a potential price puzzle.

D Robustness: Smooth Transition Local Projection

We now turn to the sensitivity of the impulse response estimates during high and low inflation regimes with respect to the specification of the smooth transition function, equation (3) in the main text.

D.1 Varying the regime switching parameter

A change of the regime switching parameter from to $\gamma = 3$ or $\gamma = 10$ does not have any significant impact on any of the impulse responses (see Figure H6 and H7).

D.2 Varying the percentile of inflation parameter

Figures H8 and H9 show that the results for both lowering c to the 70^{th} percentile of trend inflation and increasing it to the 80^{th} percentile are very similar to the baseline findings.

D.3 Using HP-Filtered PCE Inflation

Figure H10 displays the results of the smooth transition local projection with HP-filtered PCE inflation as a state variable (z_t in equation (3)). We set the smoothing parameter $\lambda = 14440$, which is the standard value for monthly data. The results are again very close to the results in the main text..

D.4 Using the trend inflation measure from Ireland (2007)

Figure H11 shows the results of the smooth transition impulse response estimation, using an alternative measure of trend inflation from the estimated DSGE model with a time-varying inflation target by Ireland (2007). We center the model-based estimate between 0 and 1 and use it as an alternative measure for the smooth transition function $F(z_t)$ in (3). The main results of the main specification still goes through, as prices react faster in a high inflation regime compared to a low regime. However, there is a significant price puzzle and output reacts significantly weaker in the low inflation regime.

E Robustness: Both tests

This section presents the results for robustness checks performed with respect to both local projection of the main text, (1) and (2).

E.1 Alternative price measure: CPI

This robustness test uses Consumer Price Index (CPI) inflation instead of PCE inflation as the inflation measure. Figure H12 and H13 provide the results for the two main local projections using the CPI measure. It is clear that the results are quite robust to this change in the inflation response variable. The only change compared to the main results is that both regime-dependent impulse response functions now exhibit a significant price puzzle.

E.2 Controlling for commodity prices

For this robustness exercise, we add two lags and the contemporaneous value of the commodity price index in the controls. This is done in order to take into account of the fact that inflation is sensitive to movements in commodities and/or oil prices. Results, depicted in Figures H14 and H15 are largely unchanged in this case.

E.3 Controlling for financial frictions

Financial frictions (Bernanke *et al.* (1999); Kiyotaki and Moore (1997)) are another prominent propagation mechanism of monetary policy shocks in the literature. Variations in financial frictions over time could then affect our estimate, making them spurious. We control for financial frictions by including the contemporaneous value and two lags of the highly informative corporate bond credit spread, introduced by Gilchrist and Zakrajsek (2012), as a proxy for financial frictions (hereafter GZ-spread). This series is available from January 1973, so we are estimating our local projection on a truncated sample.

The results, reported in Figures H16 and H17 are mostly unchanged. With respect to our first implication, we still can discern a weaker effect of large shocks on output and a more pronounced, yet less persistence response of prices. The figure for the second hypothesis shows that inflation behaves as in the baseline specification, with a statistically significantly different and quicker response in the high inflation regime compared to the low inflation regime. Yet, we do observe a stronger reaction of output in the high inflation regime. This is mostly driven by a significant output expansion and a non-significant contraction in the low inflation regime. However, if we calculate the cumulative output response as in Table 2 the cumulative output difference is statistically insignificant. Taking this into account, we conclude that our evidence in favor of a sticky price theory holds up to controlling for the presence of financial frictions.

E.4 Non-linear Romer and Romer (2004) regression

The shocks used in the main local projections are residuals of the estimated reaction function of the central bank. More specifically, Romer and Romer (2004) assume a concrete form of reaction function by regressing the change in the intended federal funds rate ($\widehat{\Delta FFR_t}$) on a measure of forecast variables primarily obtained from the Greenbook. This method assumes that the reaction function is linear. Following Tenreyro

and Thwaites (2016), we re-estimate the Romer and Romer (2004) regression using the smooth transition function of the main specification, as:

$$\widehat{\Delta FFR_t} = F(z_t)(\mathbf{X}_t\beta^H) + (1 - F(z_t))(\mathbf{X}_t\beta^L) + e_t^{NL}. \tag{E12}$$

In doing so, the identified shocks now account for the possibility that monetary authorities reacted differently to forecasts in a high and low trend inflation regime. The new series of non-linear shocks (e_t^{NL}) has a correlation of 0.92 with the linear shocks sample (see Figure H32). This suggests that, whilst the new reaction function is picking up some non-linearities, the original shocks are a good instrument. Figures H18 and H19 shows that the results are again similar to the original ones. Note that in the smooth transition local projection, output reacts significantly stronger at short horizons in the high inflation regime, but effect disappears very quickly having no significant impact on the cumulative response. Further, still see a quicker decrease of prices in that regime, reinforcing our original results.

E.5 Shocks from a smooth transition VAR

This subsection investigates the sensitivity of the results with respect to an alternative shock measure. More specifically, we use a smooth transition version of the classical three equation recursive VAR including industrial production, PCE inflation and the federal funds rate to recover the structural VAR monetary policy shocks and then use these in our local projections instead of the Romer and Romer (2004) ones.[1] The correlation of these monetary policy shocks with the Romer and Romer (2004) ones is 0.32. Moreover, they are generally much larger with a standard deviation of 1.07 compared to our standard shocks that have a standard deviation of 0.31 (see Figure H33). They

[1]We use a lag polynomial of 3, as suggested by various information criteria. This lag length is also very similar to the one used in Caggiano *et al.* (2017) where they use a non-linear VAR with a lag length of 2 months.

also exhibit much more variation across subsamples. Figure H20 and H21 are generally supporting our baseline results but there are some differences that are worth pointing out. The local projection estimates of the linear and absolute value interaction exhibit the same pattern, but they are generally weaker in magnitude. Regarding the smooth transition local projection for the second theoretical implication, the reaction of inflation in the two regimes is in line with the prior of state dependence, yet the significance of this result is weaker compared to our baseline result. The differential reaction of output is mostly insignificant, except for early horizons where output reacts stronger in a high inflation regime. The reaction of the Fed Funds rate is much stronger in the high inflation regime in the first six months, which could explain the stronger initial output response. We conclude based on this that the main conclusion of higher price flexibility in a high inflation regime still applies, especially when one considers the estimates of the inflation response.

E.6 Including leads and lags of the shocks

As shown in Alloza *et al.* (2019) it is important to account for potential persistence of narrative shocks by including leads of the shock. We follow this suggestion by re-estimating our main specifications with one lag and one lead of the shock included. The results in Figures H22, H23 are largely unchanged and consequently suggest that our results are not sensitive to the inclusion of a lag or lead structure of shocks.

E.7 Quarterly estimation using GDP as output measure

In order to check the robustness of our results with respect to the output measure, we switch to a quarterly specification of our local projections and use real GDP instead of industrial production as real GDP is measured at a quarterly frequency. The results are depicted in Figure H24 and H25. The results are very similar to our monthly baseline specification with industrial production as our output measure.

E.8 Quarterly estimation including fiscal policy controls

In order to control for the effects of fiscal policy on our estimates we also use a quarterly estimation of our local projection as most of these shocks are measured at a quarterly frequency. First, we control for government spending shocks by including two lags and the contemporaneous value of the excess returns of military contractors, popularised by Fisher and Peters (2010). These results are reported in H26 and H27. The results with respect to the absolute value interaction are basically unchanged. The results with respect to our smooth transition local projection are a bit different compared to the baseline. There is no significant difference between the two inflation impulse responses at early horizons, yet the point estimates and the significance at later horizons do support our main results. Further, we now see a stronger output response in the low inflation regime, in line with our state-dependent pricing. Second, we control for tax shocks by including two lags and the contemporaneous value of the exogenous tax series by Romer and Romer (2010) in H28 and H29. The results with respect to both tests are in line with our main results, and even somewhat better, as there is a significantly stronger reaction of industrial production in the low inflation regime.

E.9 Unsmoothed results

Figures H30 and H31 report the unsmoothed results of the benchmark non-linear and smooth transition local projections, respectively.

F Shock distribution: Asymmetries and business-cycle dependencies

Figures H32 and H33 provide the time series of the shocks used in our local projections and their respective correlations.

Recent research has documented that monetary policy shocks have different effects in booms versus recessions as well as asymmetric effects in terms of positive versus negative shocks (see Tenreyro and Thwaites, 2016; Barnichon and Matthes, 2018). Hence, it is important to analyse whether the distribution of the size of the shock and the high vs. trend inflation regime are independent of the state of the economy and the sign of the shock. Figures H34 and H35 show the state-dependent distributions of the linear Romer and Romer shocks for high- and low inflation regimes and recessions and booms, respectively.[2] First, regarding our results for high vs. low trend inflation, the high inflation regime exhibits slightly fatter tails than the low trend inflation regime, but both for positive and negative shocks. Hence, it does not seem that the results about trend inflation are due to having an asymmetric distribution of positive and negative shocks in low vs. high trend inflation regimes. Moreover, we included a dummy term for recessions in order to control for differential effects of high and low inflation responses, depending on the business cycle. The results are shown in Figure H36. It is evident that inflation reacts quicker in high inflation regimes, both during booms and recessions. This validates the robustness of our results to the state of the business cycle. Second, regarding our results for large vs. small shocks, H35 shows that the distribution of the shocks is different between recessions and booms, as already highlighted by Tenreyro and Thwaites (2016). Recessions feature large negative shocks. This complicates the identification of all these effects in US data, because recessions, negative shocks and large shocks tend to appear at the same time. As the previous cited papers that wanted to distinguish the effects of the state of the economy (recession vs. boom) from the effects of the sign of the shock (asymmetric effect), our analysis is subject to this caveat. Our specification (1), however, does control for the sign of the shock, given the presence of a quadratic term in it, as explained above. While we do find some evidence of asymmetric

[2]The average shock distribution is computed with the linear Romer and Romer shocks, smoothed with a normally distributed kernel. The high inflation and low inflation estimates are generated by weighting the kernel function with the headline smooth transition function. The boom and recession estimates are generated by weighting the kernel function with the NBER recession dates.

effects, our results are unchanged when controlling for it. Moreover, when we interact our non-linear and absolute value interaction with a dummy term for recessions we find that the shape of the point estimate is constant across regimes and the difference between these two IRF is largely insignificant (see Figure H37).

G Hansen (1992) test procedure

This description closely follows the exposition in Hansen (1992). We use the following specification in order to test for possible structural breaks in the individual impulse response coefficients:

$$y_{t+h} = \alpha_h + \beta_h \epsilon_t + \zeta_h \left(\epsilon_t \cdot |\epsilon_t|\right) + \sum_{k=1}^{K} \gamma_{h,k} w_{t,k} + v_{t+h} \equiv b_h' x_t + v_{t+h} \tag{G13}$$

and assume $E(v_{t+h}|x_t) = 0$ and $E(v_{t+h}^2) = \sigma_{t,h}$ and $\lim_{T\to\infty} \frac{1}{T} \sum_{t=1}^{T} \sigma_{t,h}^2 = \sigma_h^2$. Furthermore, the variables cannot contain any deterministic or stochastic trends. Accordingly, we modify our original specification by excluding the deterministic time trend and taking first differences of the industrial production and federal funds rate control variables to ensure the fulfillment of this assumption.

Estimating equation (G13) with ordinary least squares yields $(\hat{b}_h, \hat{\sigma}_h)$ and the following system of first-order conditions:

$$0 = \sum_{t=1}^{T} f_{k,t,h} \quad k = 1, \ldots, K+1 \tag{G14}$$

where the variables $\{f_{k,t,h}\}$ are defined as:

$$f_{k,t,h} = \begin{cases} x_{k,t} \hat{v}_{t+h} & \text{for} \quad k = 1, \ldots, K \\ (\hat{v}_{t+h}^2 - \hat{\sigma}_h) & \text{for} \quad k = K+1 \end{cases} \tag{G15}$$

where K is the number of coefficients to be estimated in the local projection. The Hansen (1992) individual test statistic is then based on the cumulative of these first order conditions. Defining the cumulative first-order condition at time t for horizon h and estimate k as $S_{k,t,h} \equiv \sum_{j=1}^{t} f_{k,j,h}$, the individual test statistic can be written as:

$$L_{k,h} = \frac{1}{T}\frac{1}{V_k}\sum_{t=1}^{T} S_{k,t,h}^2 \tag{G16}$$

where $V_k = \sum_{t=1}^{T} f_{k,t,h}^2$. This is essentially an average of squared cumulative sums of first-order conditions related to parameter k. The null hypothesis is that $b_{k,h}$ is constant and so the first-order conditions are mean zero and thus the cumulative sums wander around zero. Note that the respective distribution is non-standard and depends on the number of parameters tested for stability. The alternative is that the parameter k is not stable and will develop a non-zero mean and thus $S_{k,h}$ will be large and thus increasing the test statistic.

References

Alloza, M., Gonzalo, J. and Sanz, C. (2019). "Dynamic effects of persistent shocks", Banco de España, Working Paper.

Barnichon, R. and Brownlees, C. (2019). "Impulse Response Estimation by Smooth Local Projections", *The Review of Economics and Statistics*, vol. 101(3), pp. 522–530.

Barnichon, R. and Matthes, C. (2018). "Functional Approximation of Impulse Responses", *Journal of Monetary Economics*, vol. 99, pp. 41–55, doi:10.1016/j.jmoneco.2018.04.

Bernanke, B.S., Gertler, M. and Gilchrist, S. (1999). "The financial accelerator in a quantitative business cycle framework", in (J. B. Taylor and M. Woodford, eds.), *Handbook of Macroeconomics*, pp. 1341–1393, vol. 1 of *Handbook of Macroeconomics*, chap. 21, Elsevier.

Caggiano, G., Castelnuovo, E. and Figueres, J.M. (2017). "Economic policy uncertainty and unemployment in the United States: A nonlinear approach", *Economics Letters*, vol. 151(C), pp. 31–34.

Cover, J.P. (1992). "Asymmetric Effects of Positive and Negative Money-Supply Shocks", *The Quarterly Journal of Economics*, vol. 107(4), pp. 1261–1282.

Fisher, J.D. and Peters, R. (2010). "Using Stock Returns to Identify Government Spending Shocks", *The Economic Journal*, vol. 120(544), pp. 414–436.

Gilchrist, S. and Zakrajsek, E. (2012). "Credit Spreads and Business Cycle Fluctuations", *American Economic Review*, vol. 102(4), pp. 1692–1720.

Hansen, B.E. (1992). "Testing for parameter instability in linear models", *Journal of Policy Modeling*, vol. 14(4), pp. 517–533.

Ireland, P.N. (2007). "Changes in the Federal Reserve's Inflation Target: Causes and Consequences", *Journal of Money, Credit and Banking*, vol. 39(8), pp. 1851–1882.

Kiyotaki, N. and Moore, J. (1997). "Credit Cycles", *Journal of Political Economy*, vol. 105(2), pp. 211–248.

Newey, W.K. and West, K.D. (1987). "A Simple, Positive Semi-Definite, Heteroskedasticity and Autocorrelation Consistent Covariance Matrix", *Econometrica*, vol. 55(3), pp. 703–708.

Racine, J. (1997). "Feasible Cross-Validatory Model Selection for General Stationary Processes", *Journal of Applied Econometrics*, vol. 12(2), pp. 169–179.

Romer, C.D. and Romer, D.H. (2004). "A New Measure of Monetary Shocks: Derivation and Implications", *American Economic Review*, vol. 94(4), pp. 1055–1084.

Romer, C.D. and Romer, D.H. (2010). "The Macroeconomic Effects of Tax Changes: Estimates Based on a New Measure of Fiscal Shocks", *American Economic Review*, vol. 100(3), pp. 763–801.

Tenreyro, S. and Thwaites, G. (2016). "Pushing on a String: US Monetary Policy Is Less Powerful in Recessions", *American Economic Journal: Macroeconomics*, vol. 8(4), pp. 43–74.

H Figures

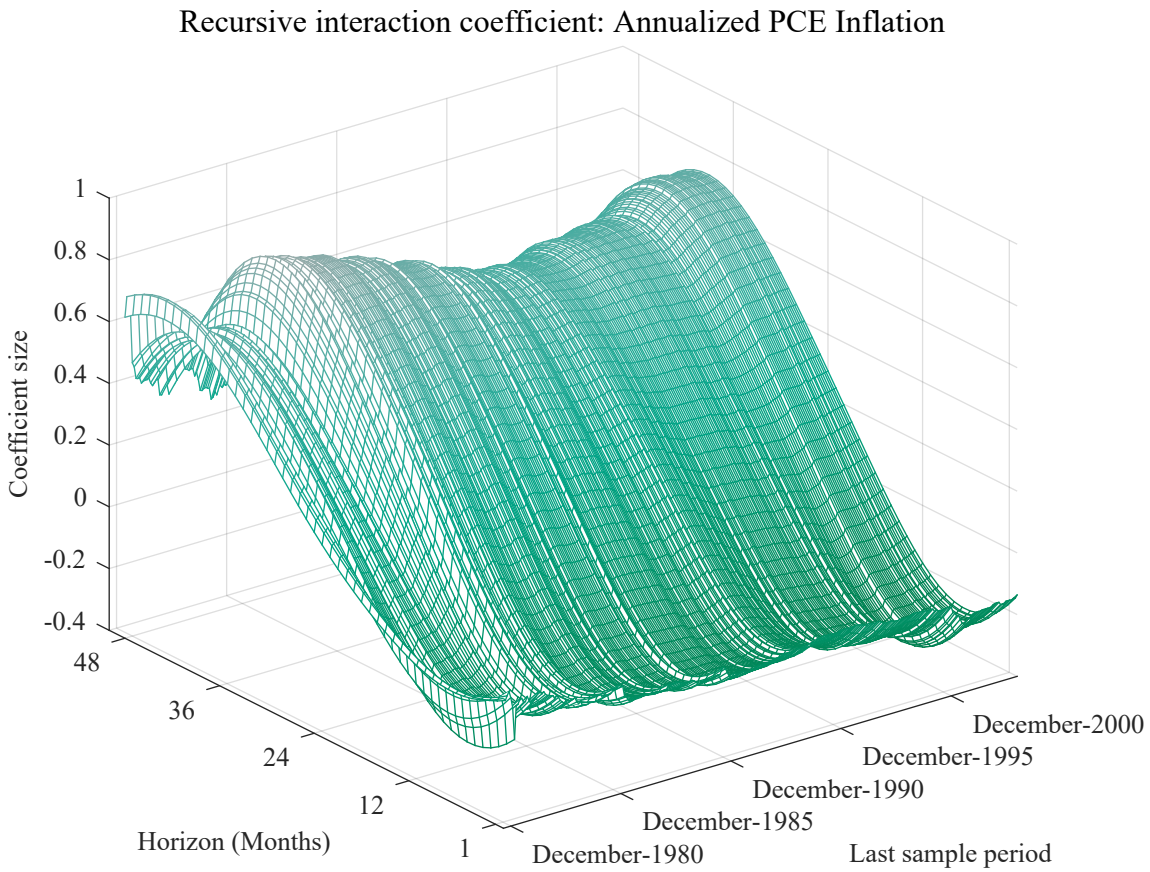

Figure H1: Recursive smooth PCE inflation local projection: absolute value interaction coefficient. The x-axis indicates the horizon of the impulse response, the y-axis indicates the last period of that estimate and the z-axis indicates the coefficient. The first sample contains the data between January 1969 and August 1980 whilst the last sample contains data between January 1969 and December 2003.

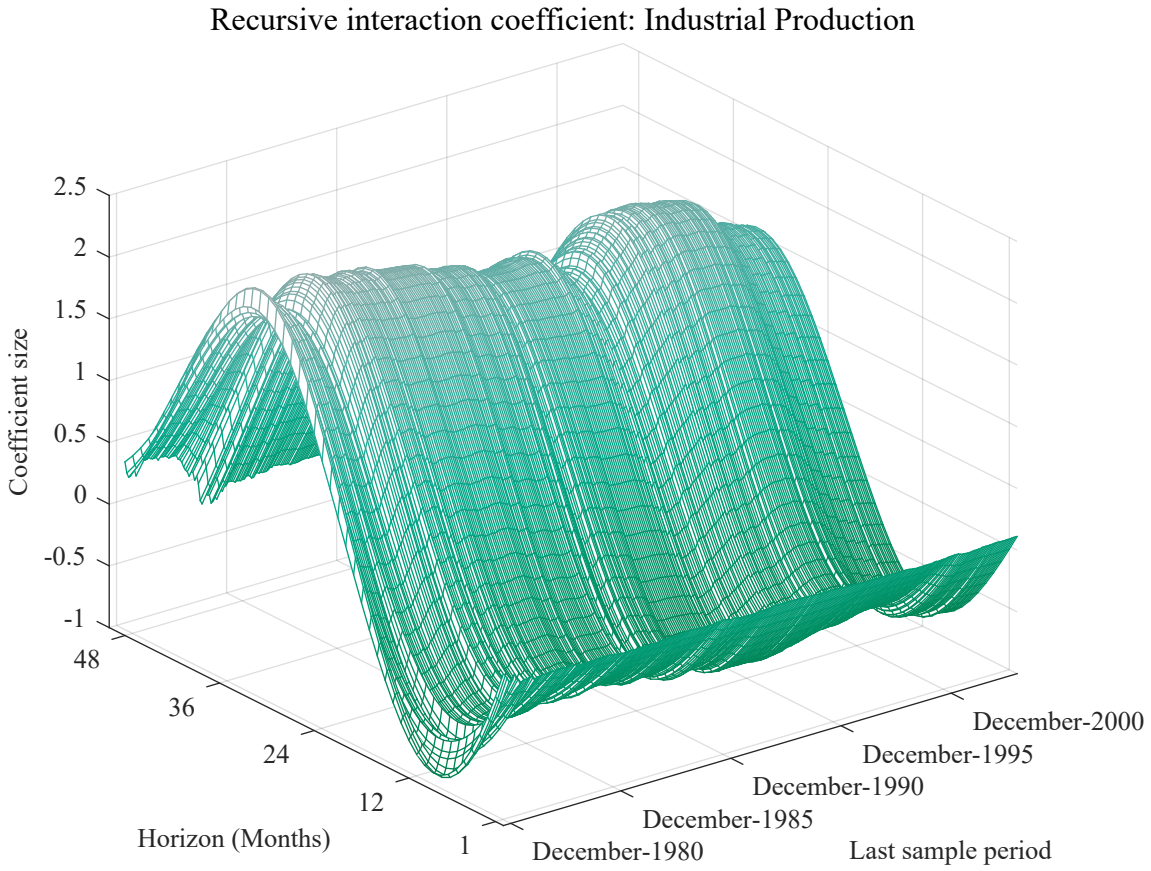

Figure H2: Recursive smooth industrial output local projection: absolute value interaction coefficient. The x-axis indicates the horizon of the impulse response, the y-axis indicates the last period of that estimate and the z-axis indicates the coefficient. The first sample contains the data between January 1969 and August 1980 whilst the last sample contains data between January 1969 and December 2003.

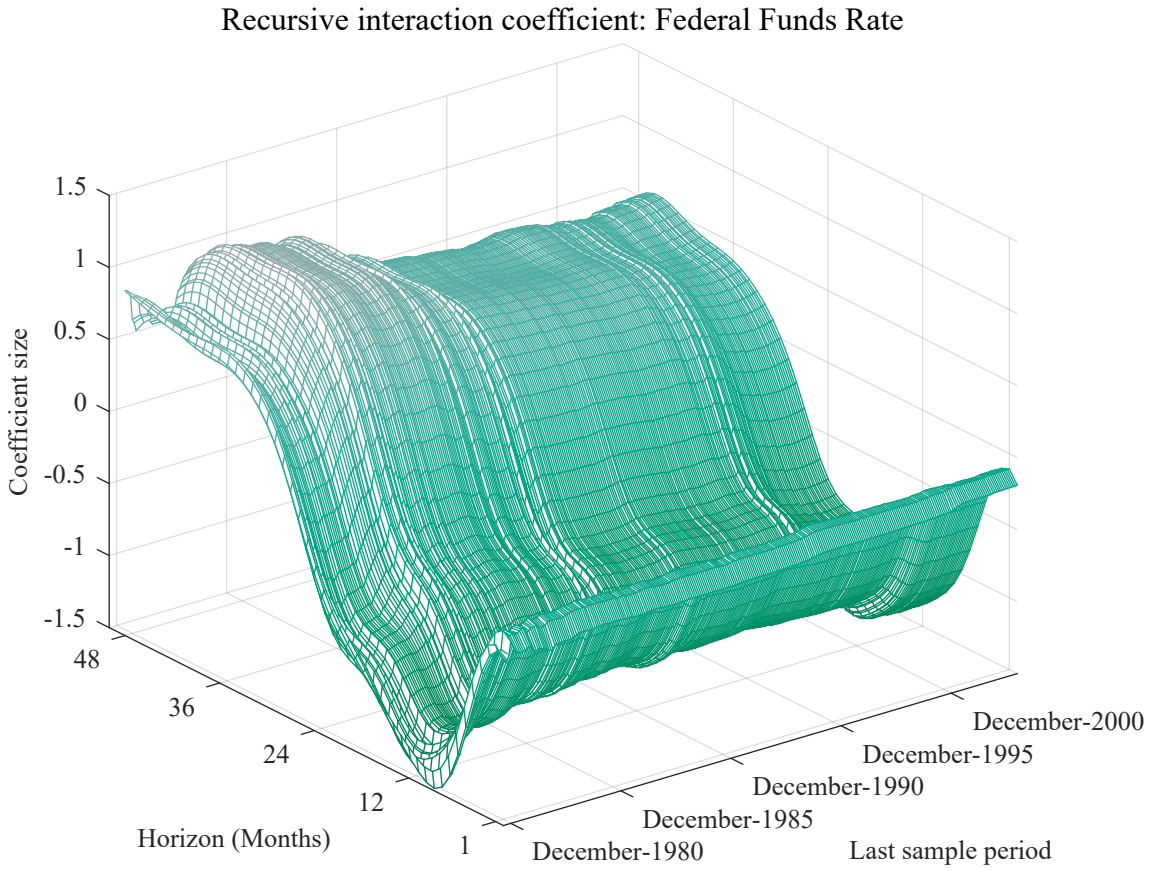

Figure H3: Recursive smooth federal funds rate local projection: absolute value interaction coefficient. The x-axis indicates the horizon of the impulse response, the y-axis indicates the last period of that estimate and the z-axis indicates the coefficient. The first sample contains the data between January 1969 and August 1980 whilst the last sample contains data between January 1969 and December 2003.

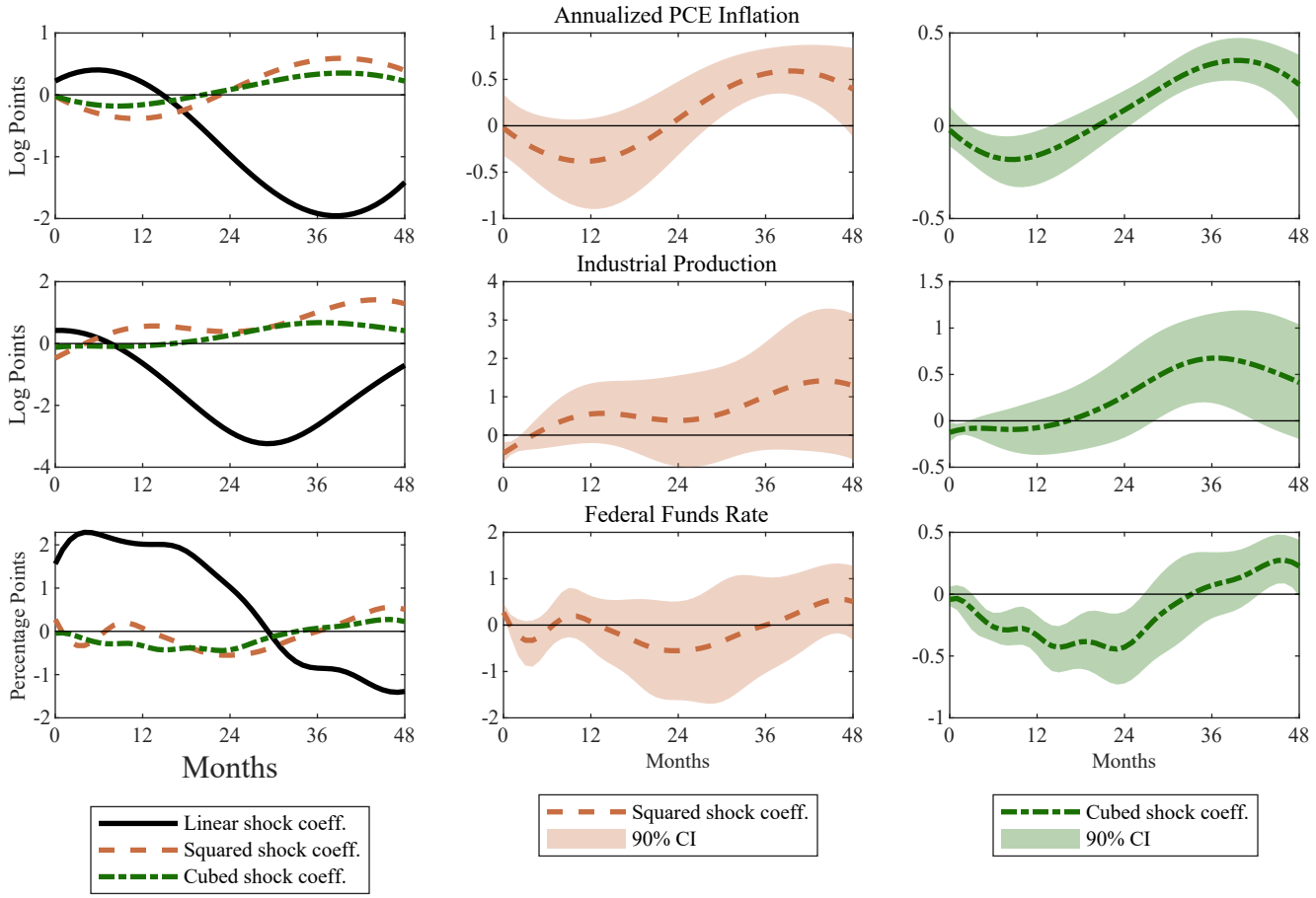

Figure H4: Panel of smooth local projection coefficients for annualized PCE inflation (first row), industrial production (second row) and the federal funds rate (third row). The first column depicts the point estimate with respect to the shock (black, solid line), its squared value (red, dashed line) and its cubed value (green, dashed-dotted line). The second column depicts the point estimate of the squared value again, together with its 90% confidence interval. The third column depicts the point estimate of the cubed value again, together with its 90% confidence interval. All of the coefficients are depicted over a four year horizon.

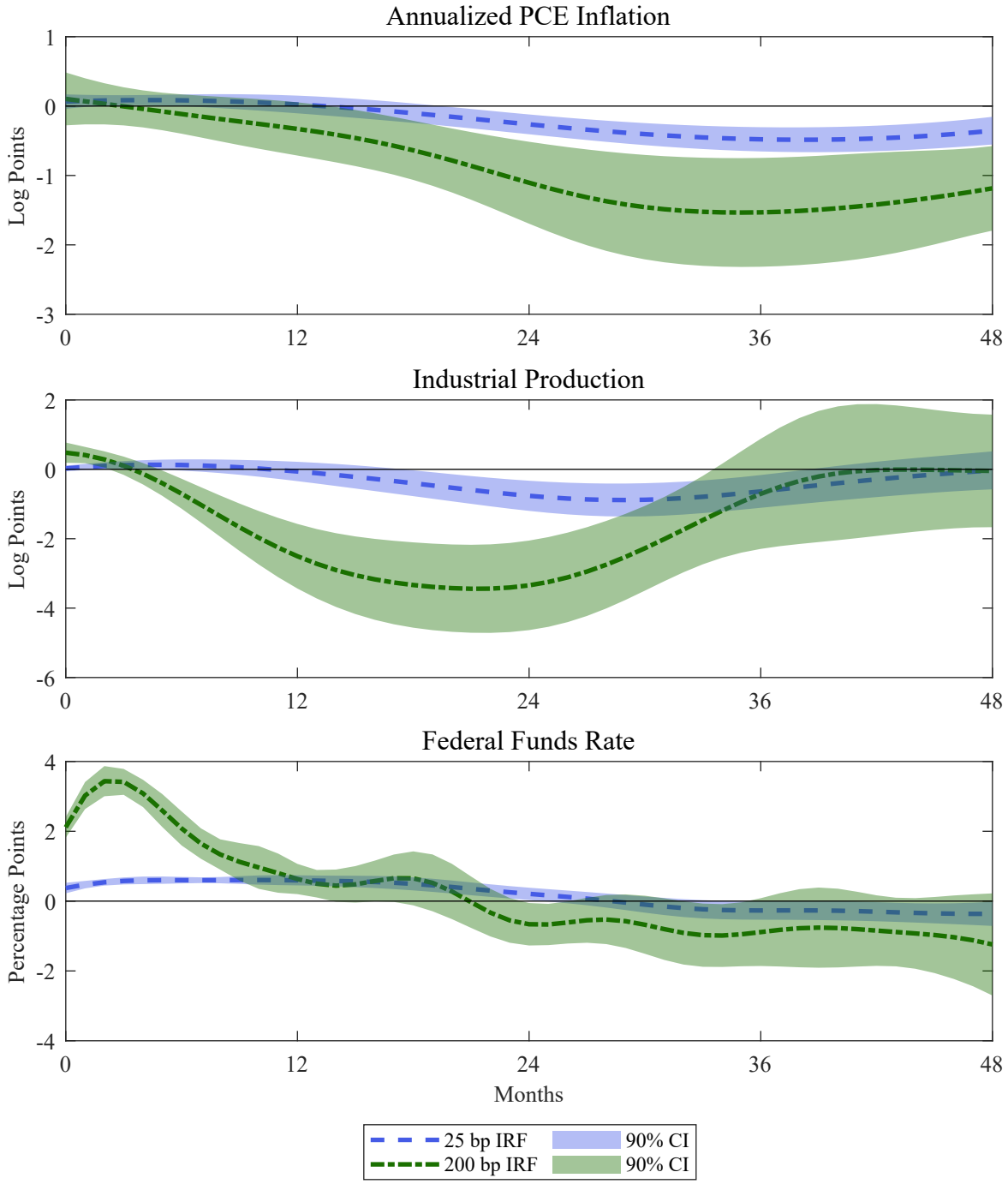

Figure H5: Panel of simulated size-dependent impulse responses for annualised PCE Inflation, Industrial Production and the Federal Funds Rate over a four year horizon. The Figure depicts the impulse response for a 25 (dashed line) and 200 (dashed-dotted) basis point shock. The impulse responses are depicted over a four year horizon.

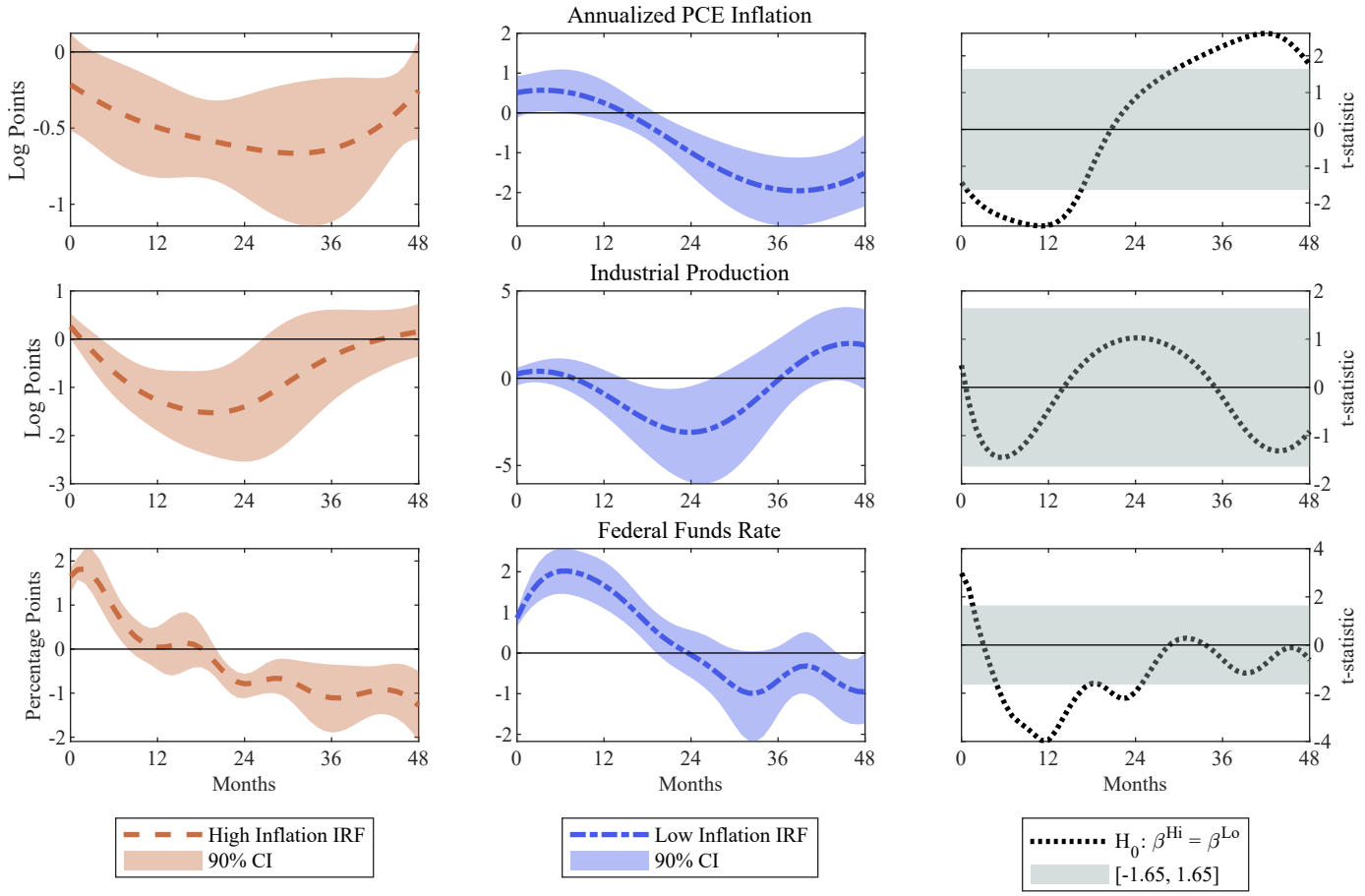

Figure H6: Panel of smooth impulse response functions in different inflation states with a lower speed of transition ($\gamma = 3$). The three response variables are annualized PCE Inflation (first row), industrial output (second row) and the federal funds rate (third row). The first column depicts the point estimates of the high inflation impulse response (dashed line) together with its 90% confidence interval. The second column depicts the point estimates of the low inflation impulse response (dashed-dotted line) together with its 90% confidence interval. The third column depicts the t-statistic for the null hypothesis of equality of the high and low inflation impulse responses (dotted line), together with the 90% z-values (grey area). All of the coefficients are depicted over a four year horizon.

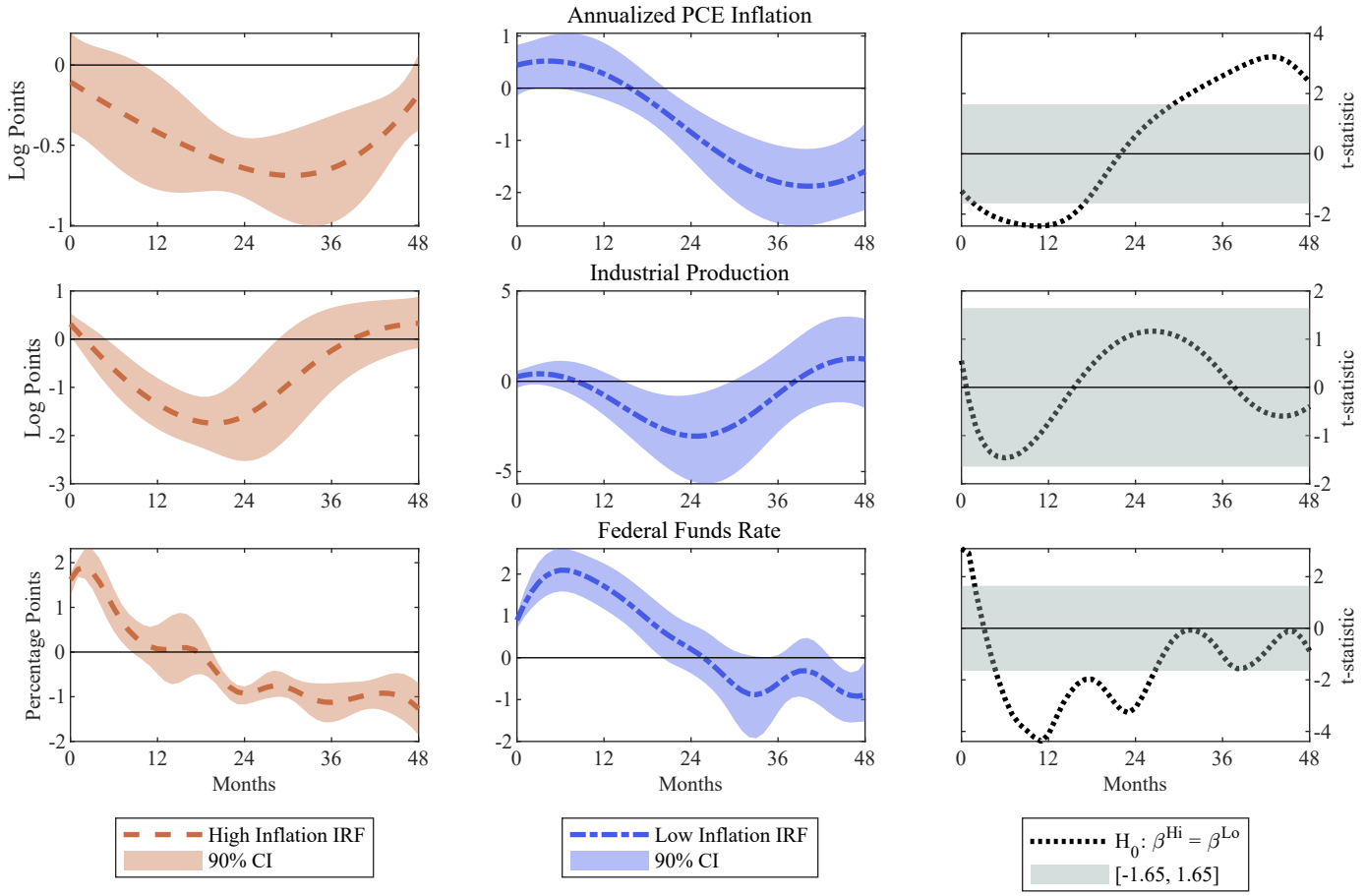

Figure H7: Panel of smooth impulse response functions in different inflation states with a higher speed of transition ($\gamma = 10$). The three response variables are annualized PCE Inflation (first row), industrial output (second row) and the federal funds rate (third row). The first column depicts the point estimates of the high inflation impulse response (dashed line) together with its 90% confidence interval. The second column depicts the point estimates of the low inflation impulse response (dashed-dotted line) together with its 90% confidence interval. The third column depicts the t-statistic for the null hypothesis of equality of the high and low inflation impulse responses (dotted line), together with the 90% z-values (grey area). All of the coefficients are depicted over a four year horizon.

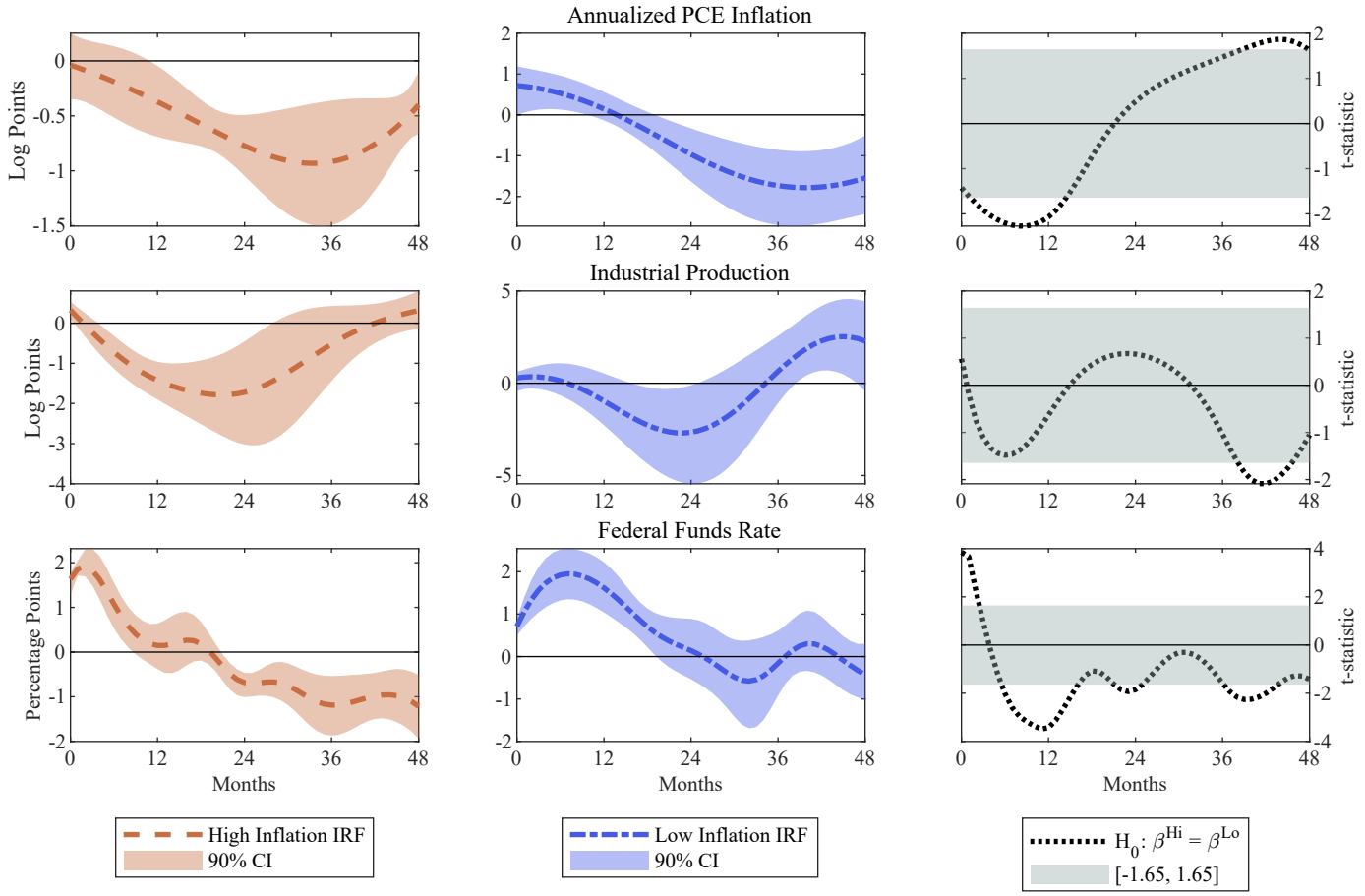

Figure H8: Panel of smooth impulse response functions in different inflation states with a lower inflation threshold ($c = 0.7$). The three response variables are annualized PCE Inflation (first row), industrial output (second row) and the federal funds rate (third row). The first column depicts the point estimates of the high inflation impulse response (dashed line) together with its 90% confidence interval. The second column depicts the point estimates of the low inflation impulse response (dashed-dotted line) together with its 90% confidence interval. The third column depicts the t-statistic for the null hypothesis of equality of the high and low inflation impulse responses (dotted line), together with the 90% z-values (grey area). All of the coefficients are depicted over a four year horizon.

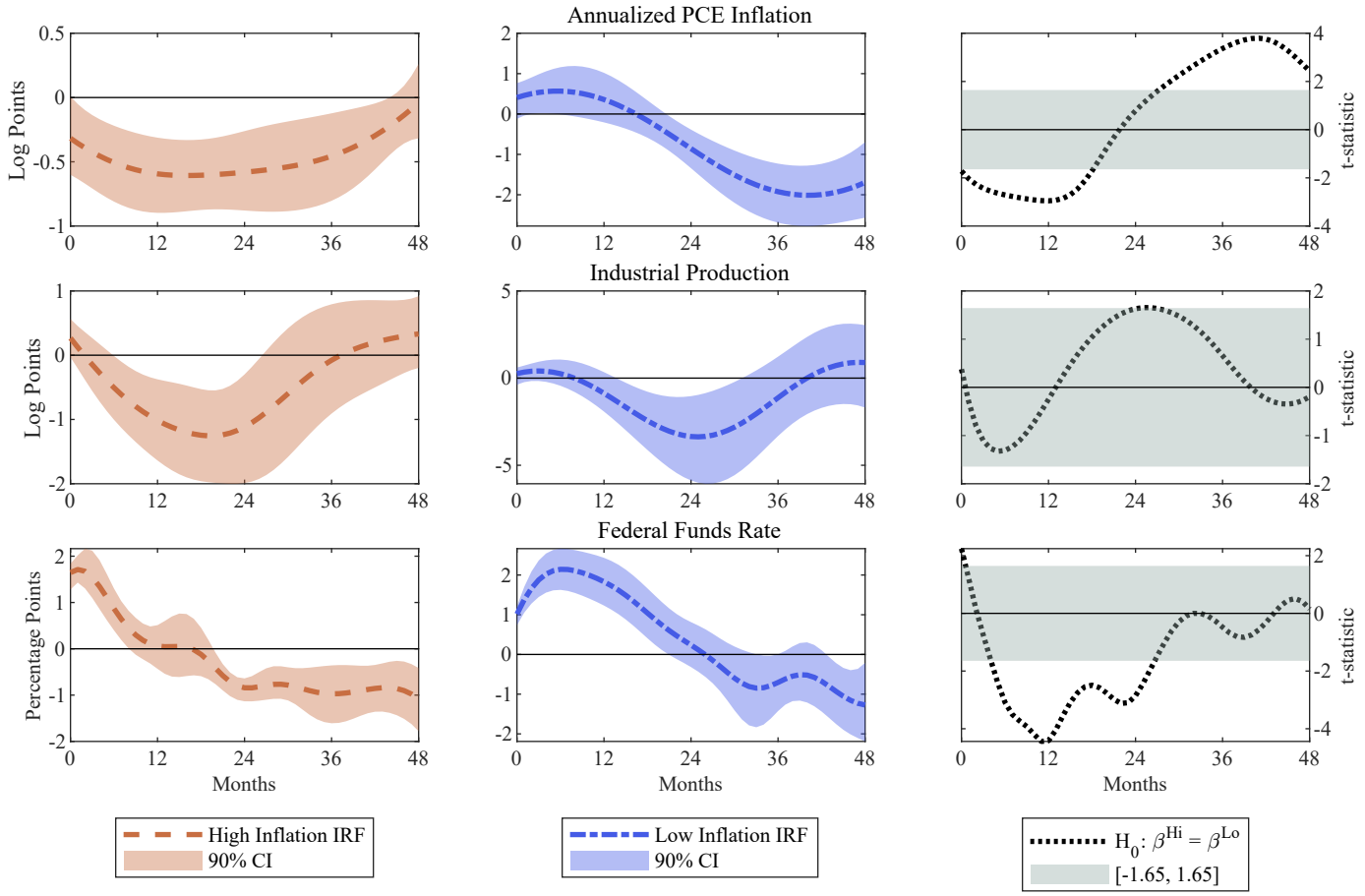

Figure H9: Panel of smooth impulse response functions in different inflation states with a lower inflation threshold ($c = 0.8$). The three response variables are annualized PCE Inflation (first row), industrial output (second row) and the federal funds rate (third row). The first column depicts the point estimates of the high inflation impulse response (dashed line) together with its 90% confidence interval. The second column depicts the point estimates of the low inflation impulse response (dashed-dotted line) together with its 90% confidence interval. The third column depicts the t-statistic for the null hypothesis of equality of the high and low inflation impulse responses (dotted line), together with the 90% z-values (grey area). All of the coefficients are depicted over a four year horizon.

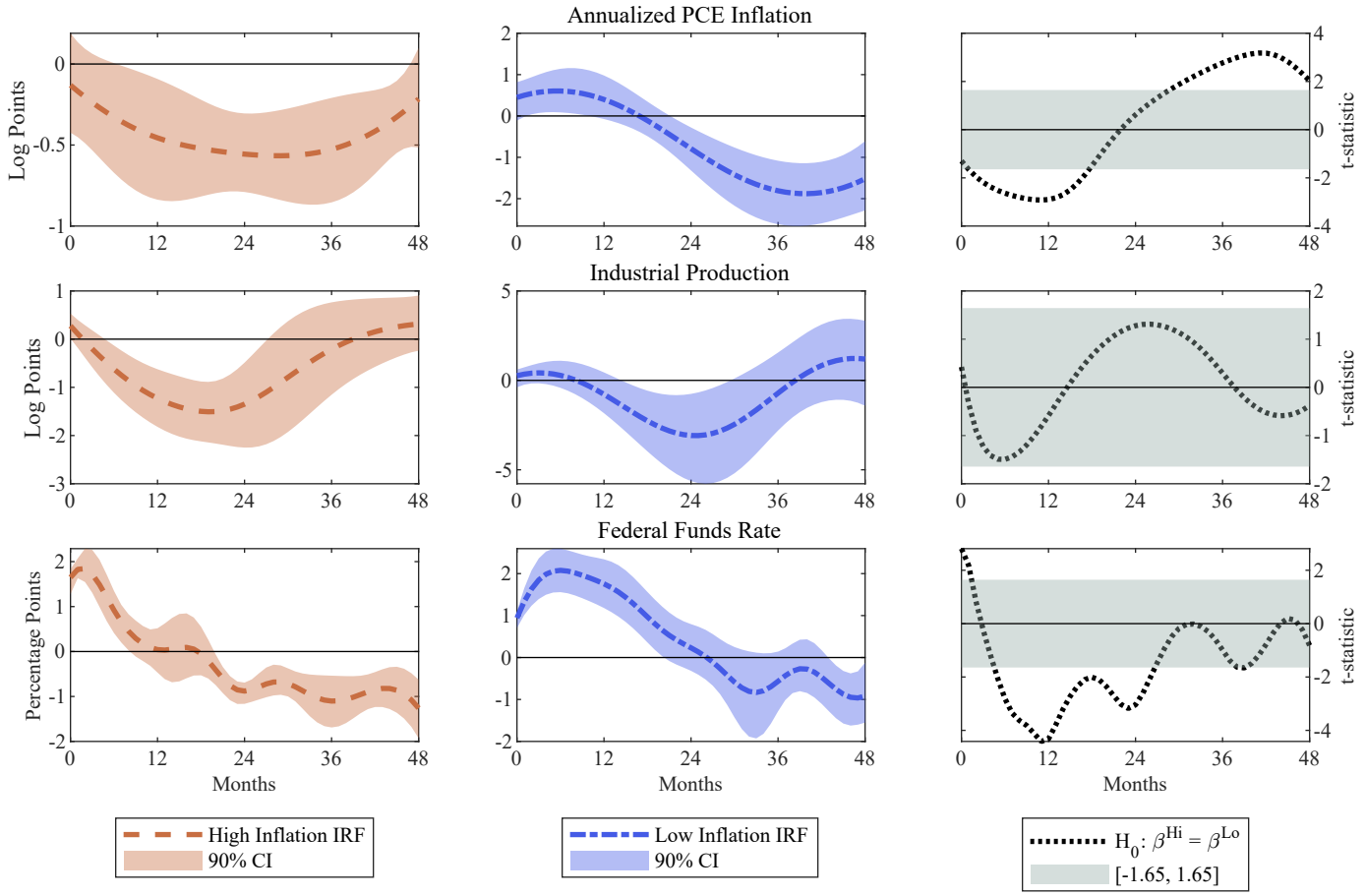

Figure H10: Panel of smooth impulse response functions in different inflation states with a HP-filtered PCE inflation as its state variable ($\lambda = 14400$). The three response variables are annualized PCE Inflation (first row), industrial output (second row) and the federal funds rate (third row). The first column depicts the point estimates of the high inflation impulse response (dashed line) together with its 90% confidence interval. The second column depicts the point estimates of the low inflation impulse response (dashed-dotted line) together with its 90% confidence interval. The third column depicts the t-statistic for the null hypothesis of equality of the high and low inflation impulse responses (dotted line), together with the 90% z-values (grey area). All of the coefficients are depicted over a four year horizon.

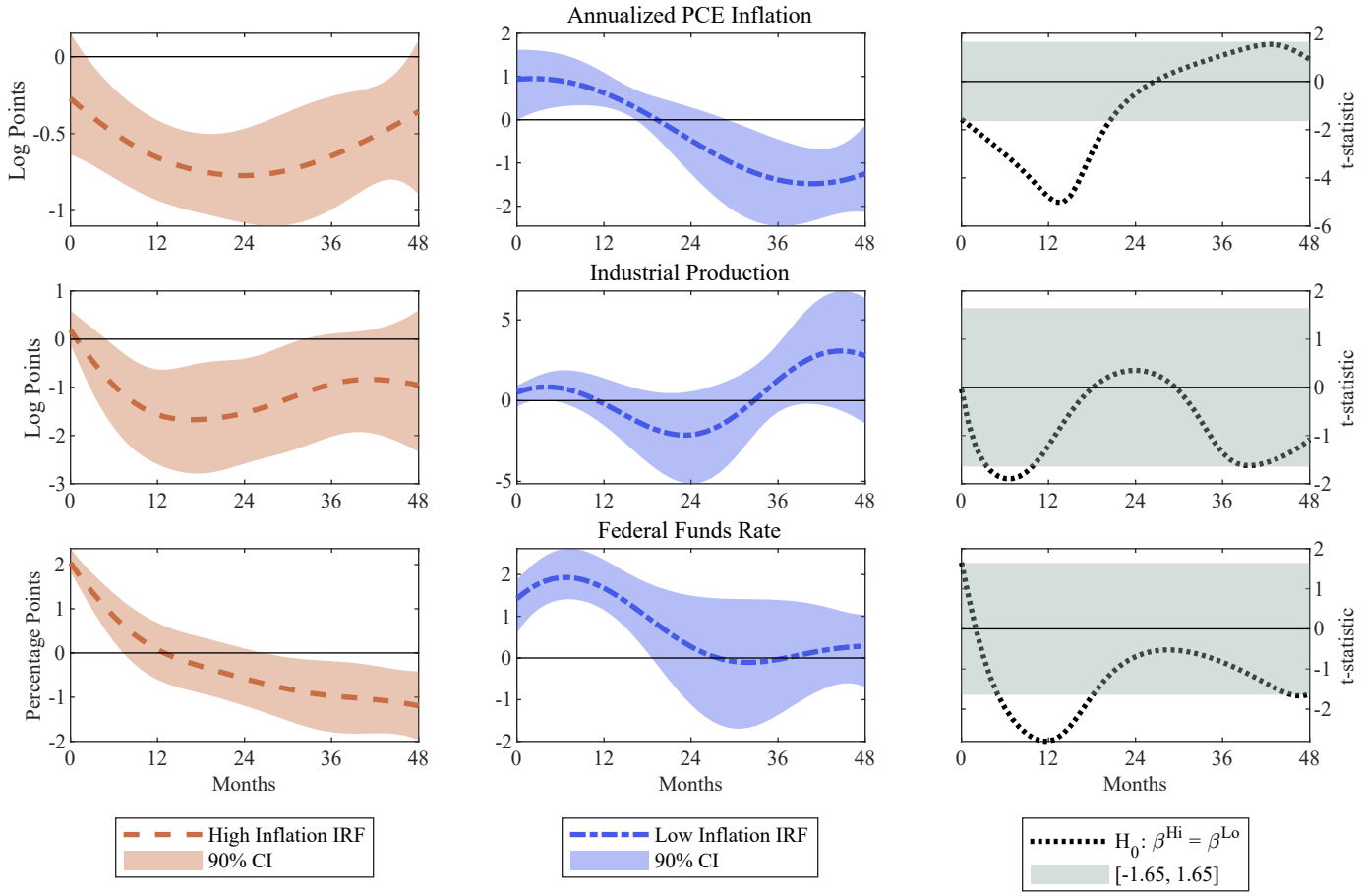

Figure H11: Panel of smooth impulse response functions in different inflation states with Peter Ireland's (2007) measure of trend inflation. The three response variables are annualized PCE Inflation (first row), industrial output (second row) and the federal funds rate (third row). The first column depicts the point estimates of the high inflation impulse response (dashed line) together with its 90% confidence interval. The second column depicts the point estimates of the low inflation impulse response (dashed-dotted line) together with its 90% confidence interval. The third column depicts the t-statistic for the null hypothesis of equality of the high and low inflation impulse responses (dotted line), together with the 90% z-values (grey area). All of the coefficients are depicted over a four year horizon.

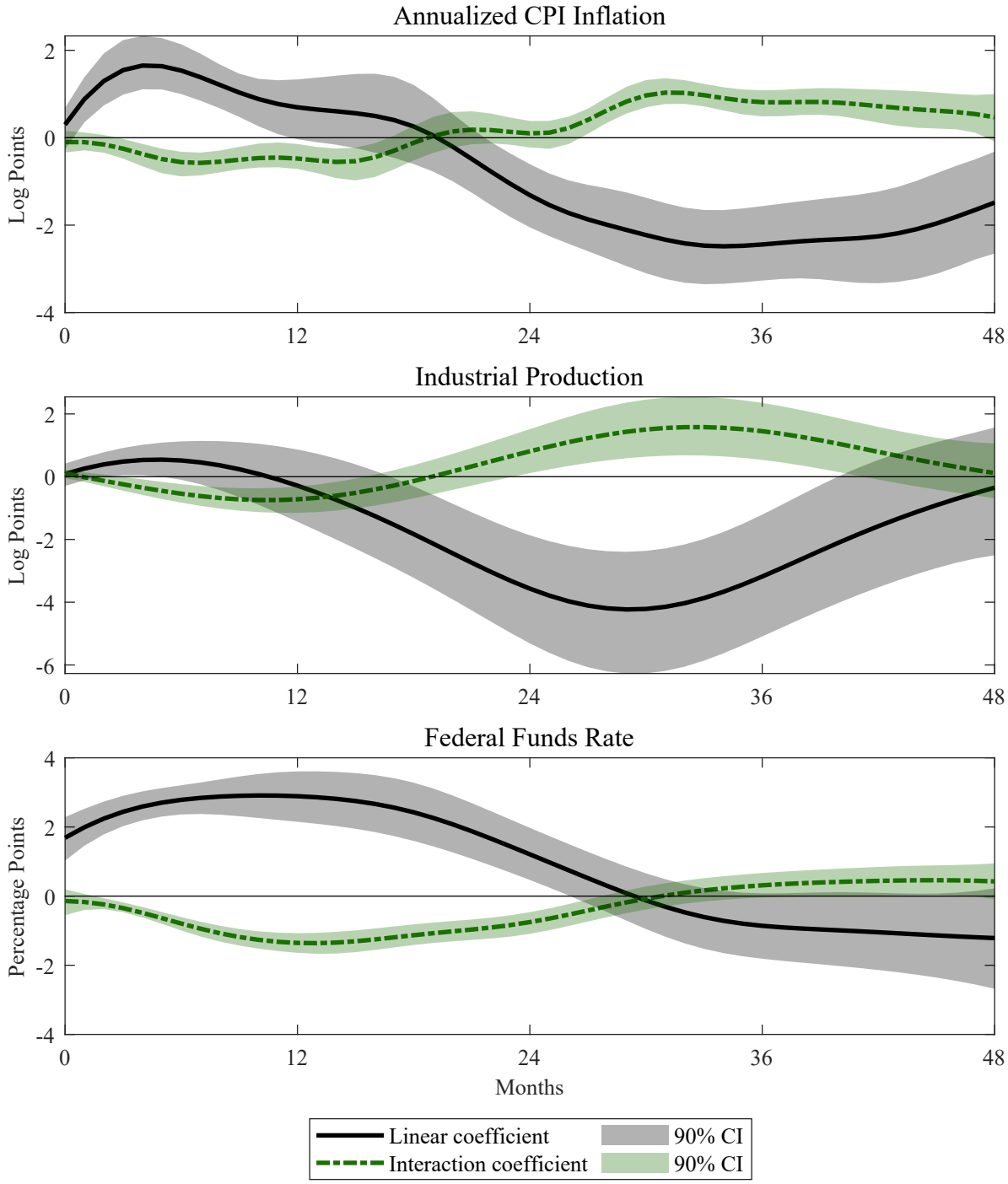

Figure H12: Panel of smooth local projection coefficients with annualized CPI inflation as the price measure. The three response variables are annualized CPI Inflation, industrial output and the federal funds rate. Every row depicts both the point estimates of the linear coefficient (solid line) and the absolute value interaction coefficient (dashed-dotted), together with their 90% confidence intervals for the various response variables. All of the coefficients are depicted over a four year horizon.

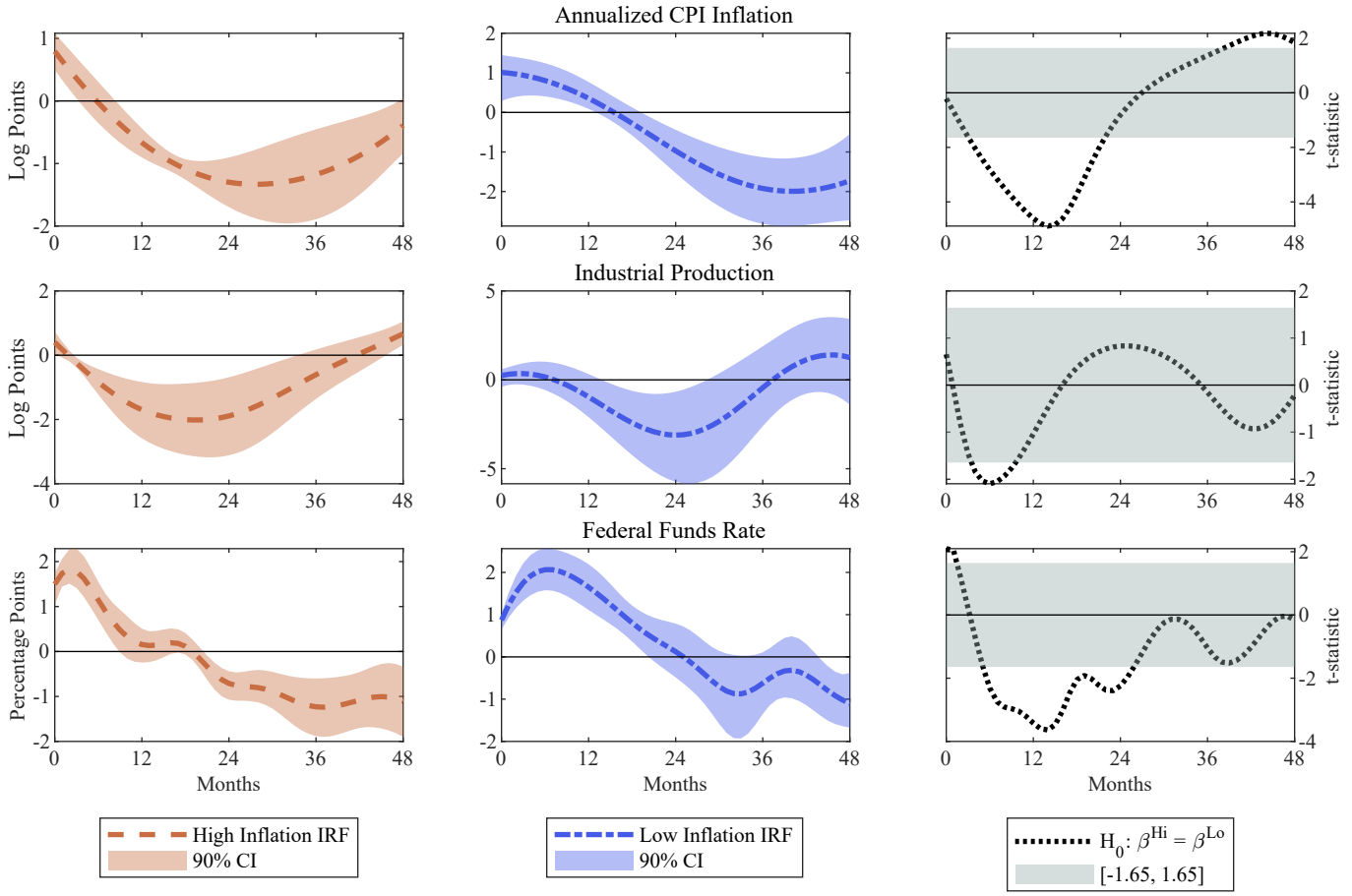

Figure H13: Panel of smooth impulse response functions in different inflation states with annualised CPI inflation as its price measure. The three response variables are annualized CPI Inflation (first row), industrial output (second row) and the federal funds rate (third row). The first column depicts the point estimates of the high inflation impulse response (dashed line) together with its 90% confidence interval. The second column depicts the point estimates of the low inflation impulse response (dashed-dotted line) together with its 90% confidence interval. The third column depicts the t-statistic for the null hypothesis of equality of the high and low inflation impulse responses (dotted line), together with the 90% z-values (grey area). All of the coefficients are depicted over a four year horizon.

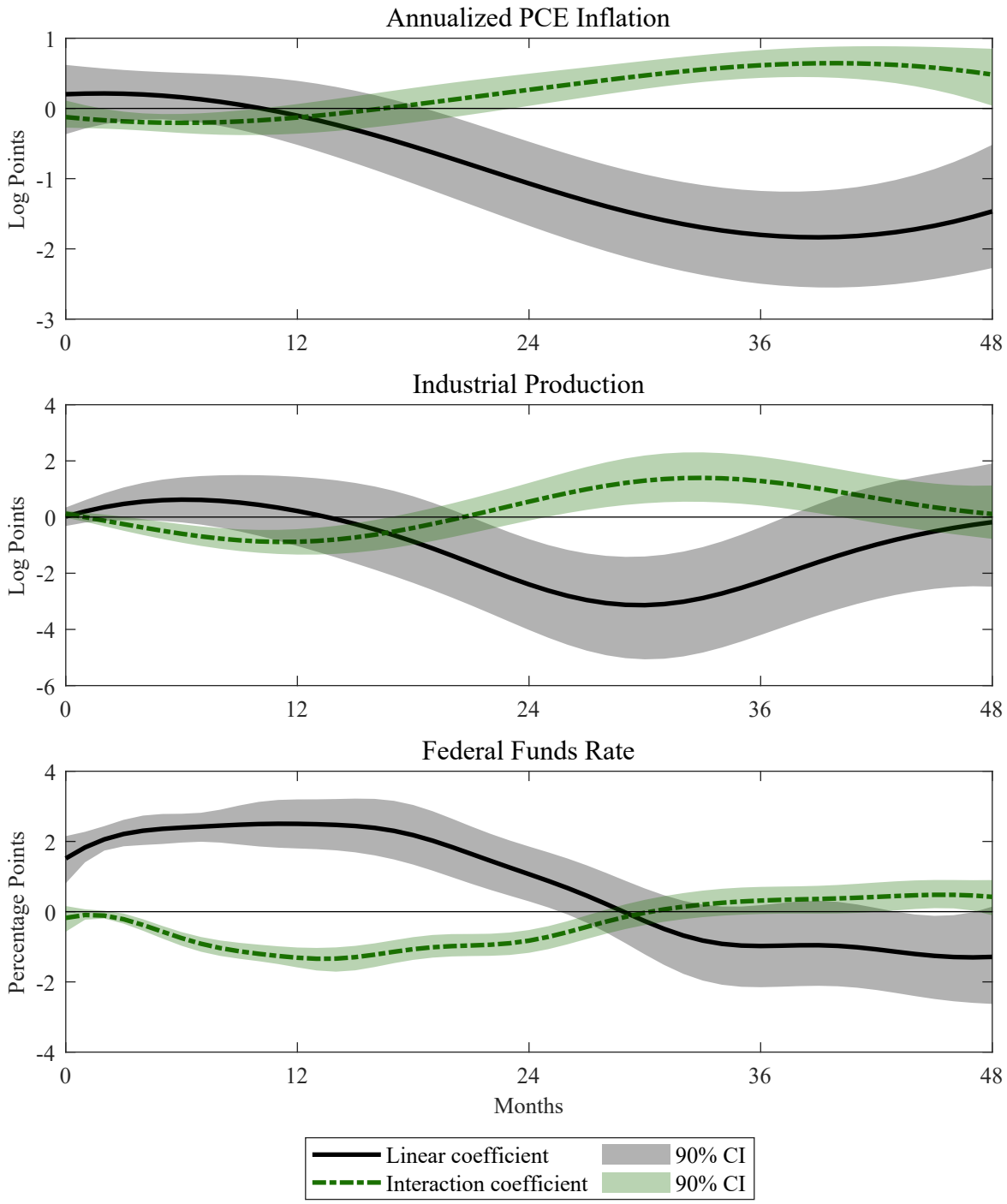

Figure H14: Panel of smooth local projection coefficients, controlling for the commercial price index (PCOM). The three response variables are annualized PCE Inflation, industrial output and the federal funds rate. Every row depicts both the point estimates of the linear coefficient (solid line) and the absolute value interaction coefficient (dashed-dotted), together with their 90% confidence intervals for the various response variables. All of the coefficients are depicted over a four year horizon.

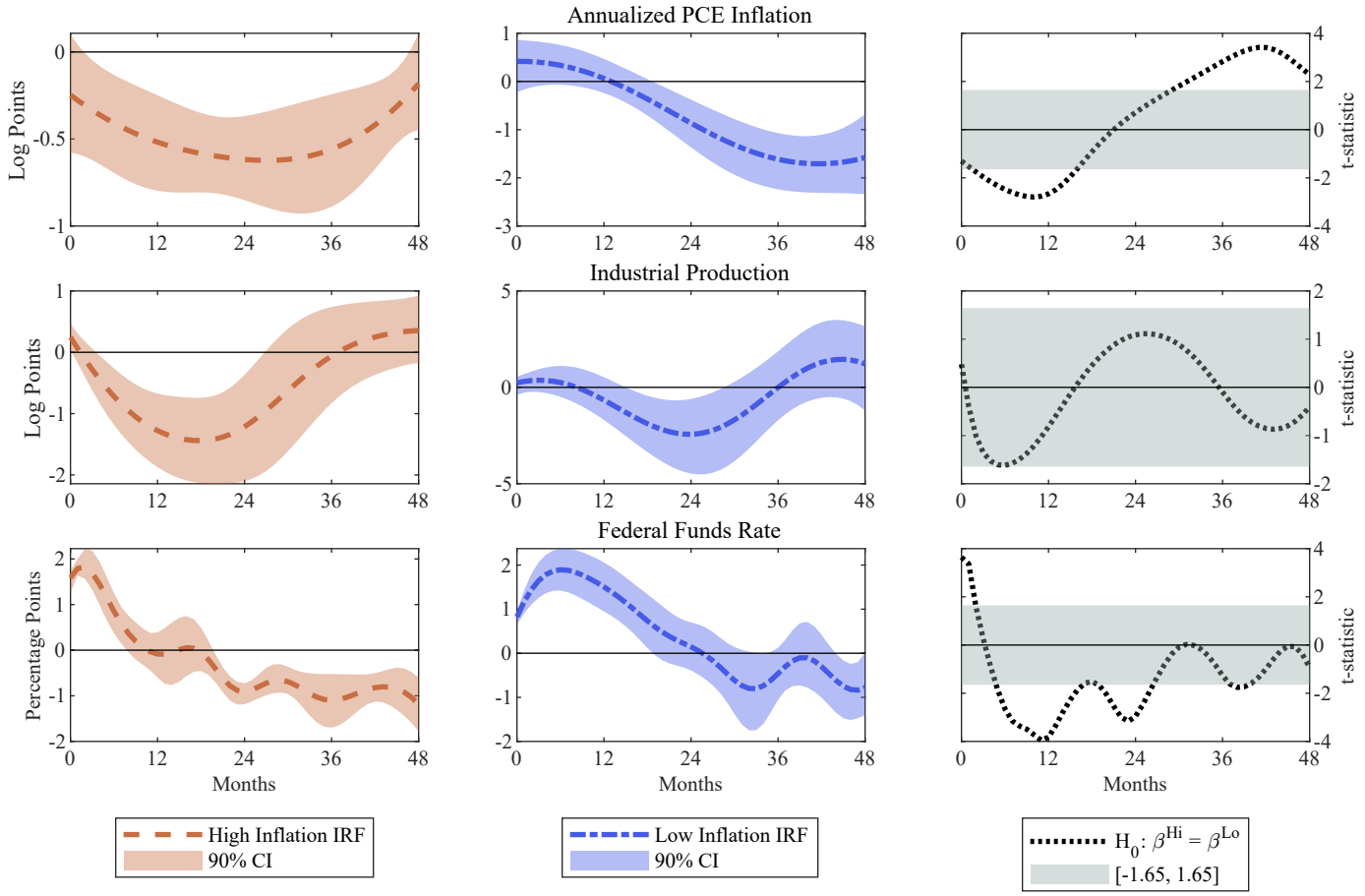

Figure H15: Panel of smooth impulse response functions in different inflation states, controlling for the commercial price index (PCOM). The three response variables are annualized PCE Inflation (first row), industrial output (second row) and the federal funds rate (third row). The first column depicts the point estimates of the high inflation impulse response (dashed line) together with its 90% confidence interval. The second column depicts the point estimates of the low inflation impulse response (dashed-dotted line) together with its 90% confidence interval. The third column depicts the t-statistic for the null hypothesis of equality of the high and low inflation impulse responses (dotted line), together with the 90% z-values (grey area). All of the coefficients are depicted over a four year horizon.

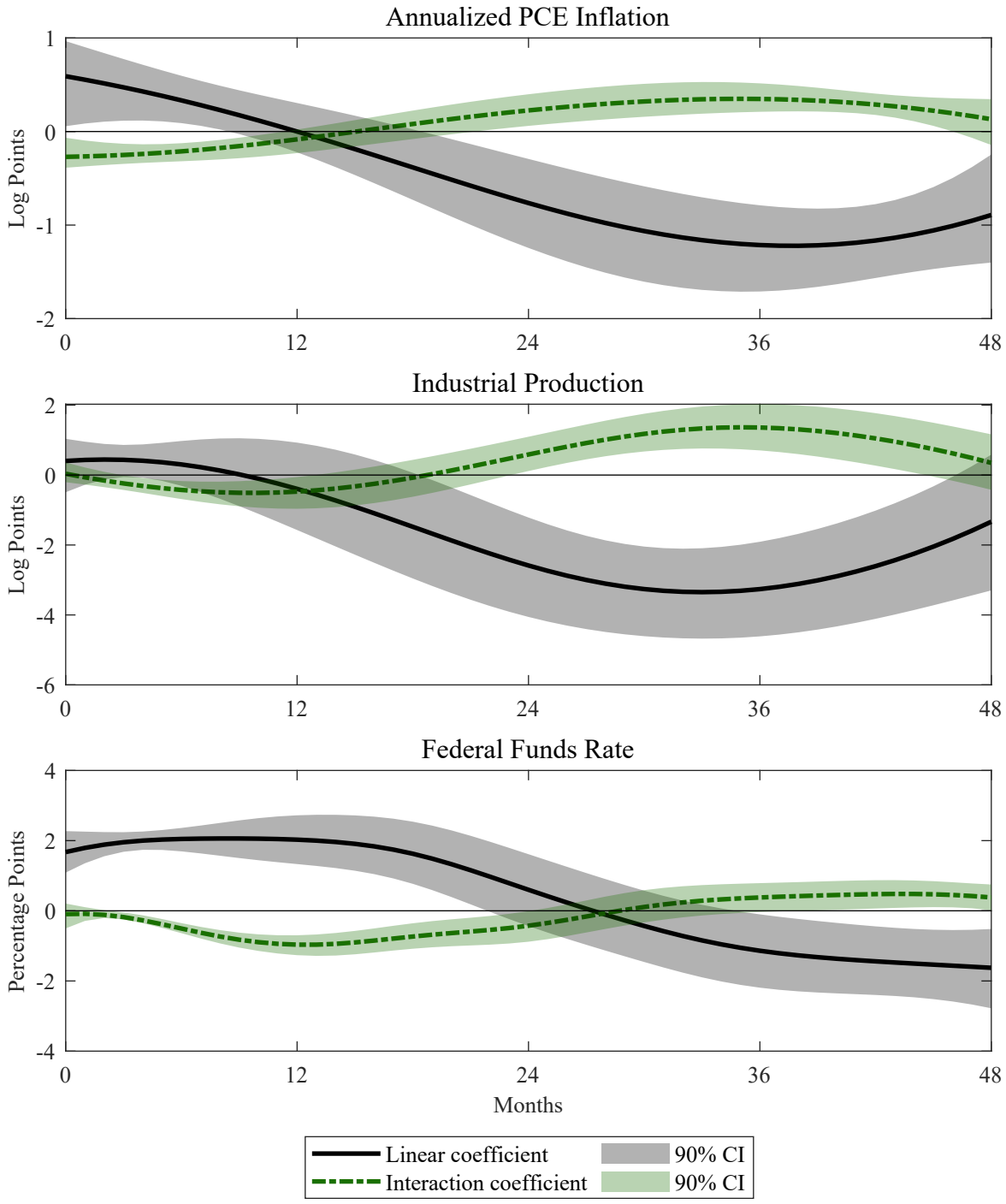

Figure H16: Panel of smooth local projection coefficients, controlling for the Gilchrist and Zakrajsek (2012) index, starting in January 1973. The three response variables are annualized PCE Inflation, industrial output and the federal funds rate. Every row depicts both the point estimates of the linear coefficient (solid line) and the absolute value interaction coefficient (dashed-dotted), together with their 90% confidence intervals for the various response variables. All of the coefficients are depicted over a four year horizon.

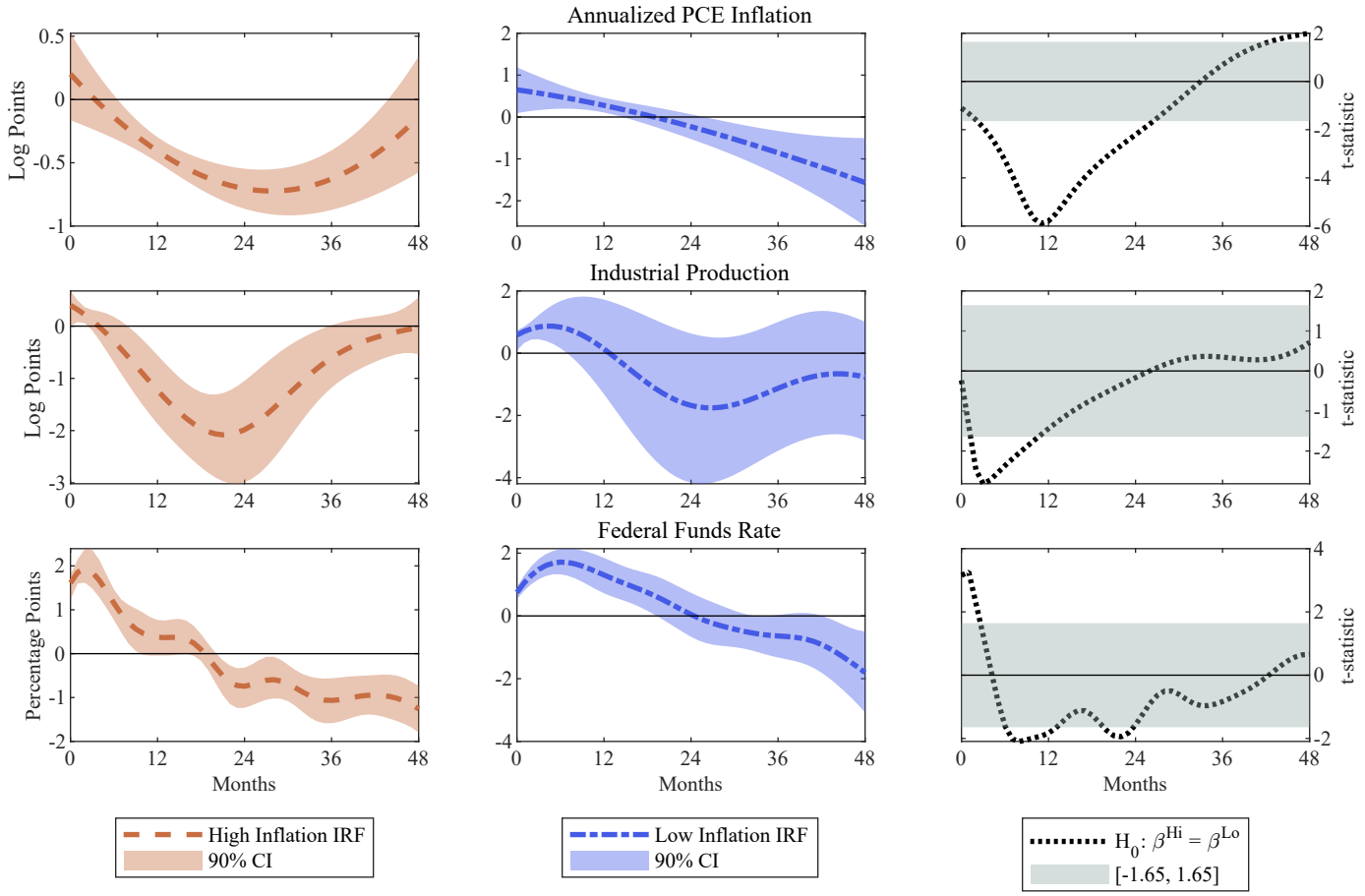

Figure H17: Panel of smooth impulse response functions in different inflation states, controlling for the Gilchrist and Zakrajsek (2012) index, starting in January 1973. The three response variables are annualized PCE Inflation (first row), industrial output (second row) and the federal funds rate (third row). The first column depicts the point estimates of the high inflation impulse response (dashed line) together with its 90% confidence interval. The second column depicts the point estimates of the low inflation impulse response (dashed-dotted line) together with its 90% confidence interval. The third column depicts the t-statistic for the null hypothesis of equality of the high and low inflation impulse responses (dotted line), together with the 90% z-values (grey area). All of the coefficients are depicted over a four year horizon.

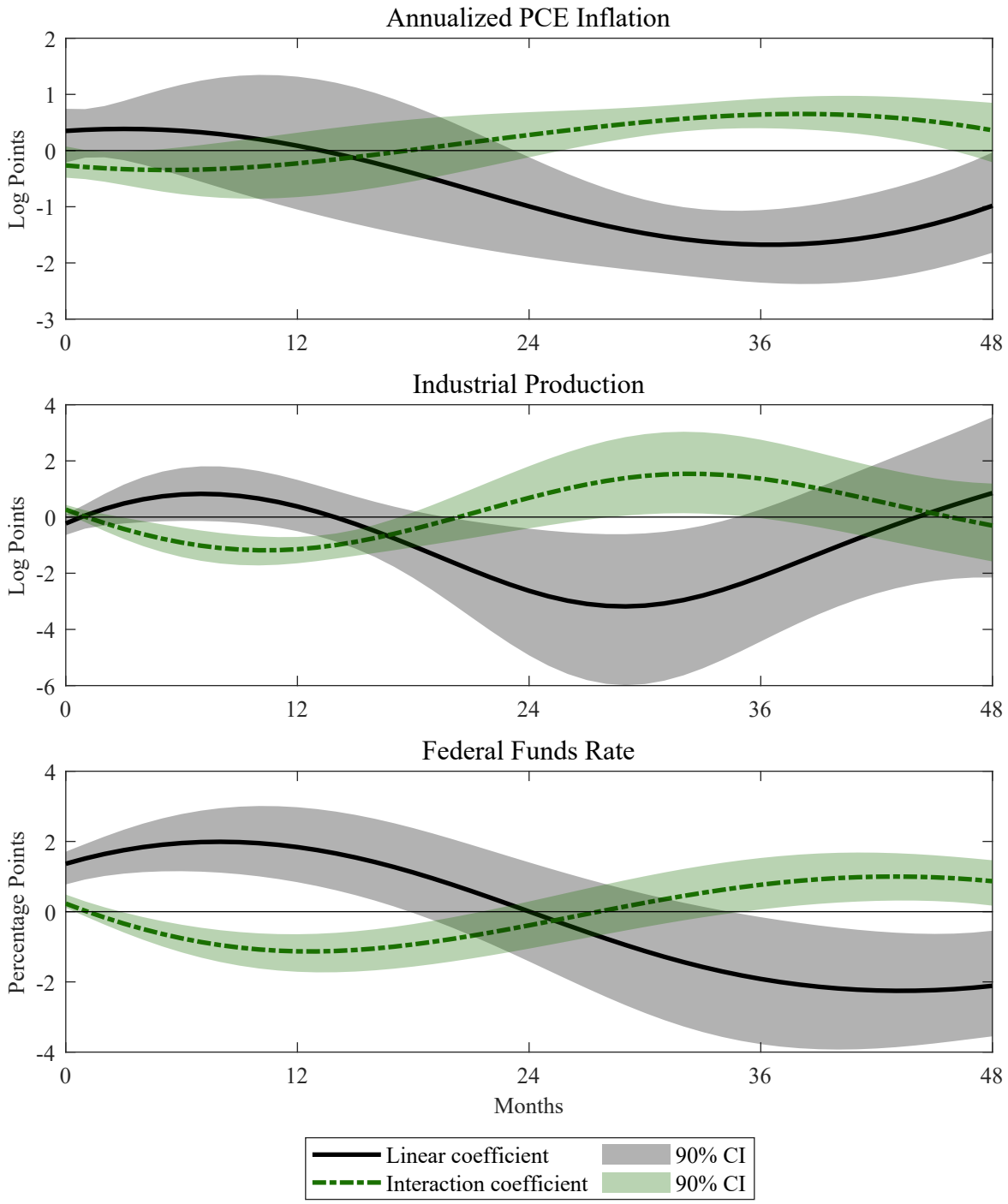

Figure H18: Panel of smooth local projection coefficients, using non-linearly identified Romer and Romer shocks. The three response variables are annualized PCE Inflation, industrial output and the federal funds rate. Every row depicts both the point estimates of the linear coefficient (solid line) and the absolute value interaction coefficient (dashed-dotted), together with their 90% confidence intervals for the various response variables. All of the coefficients are depicted over a four year horizon.

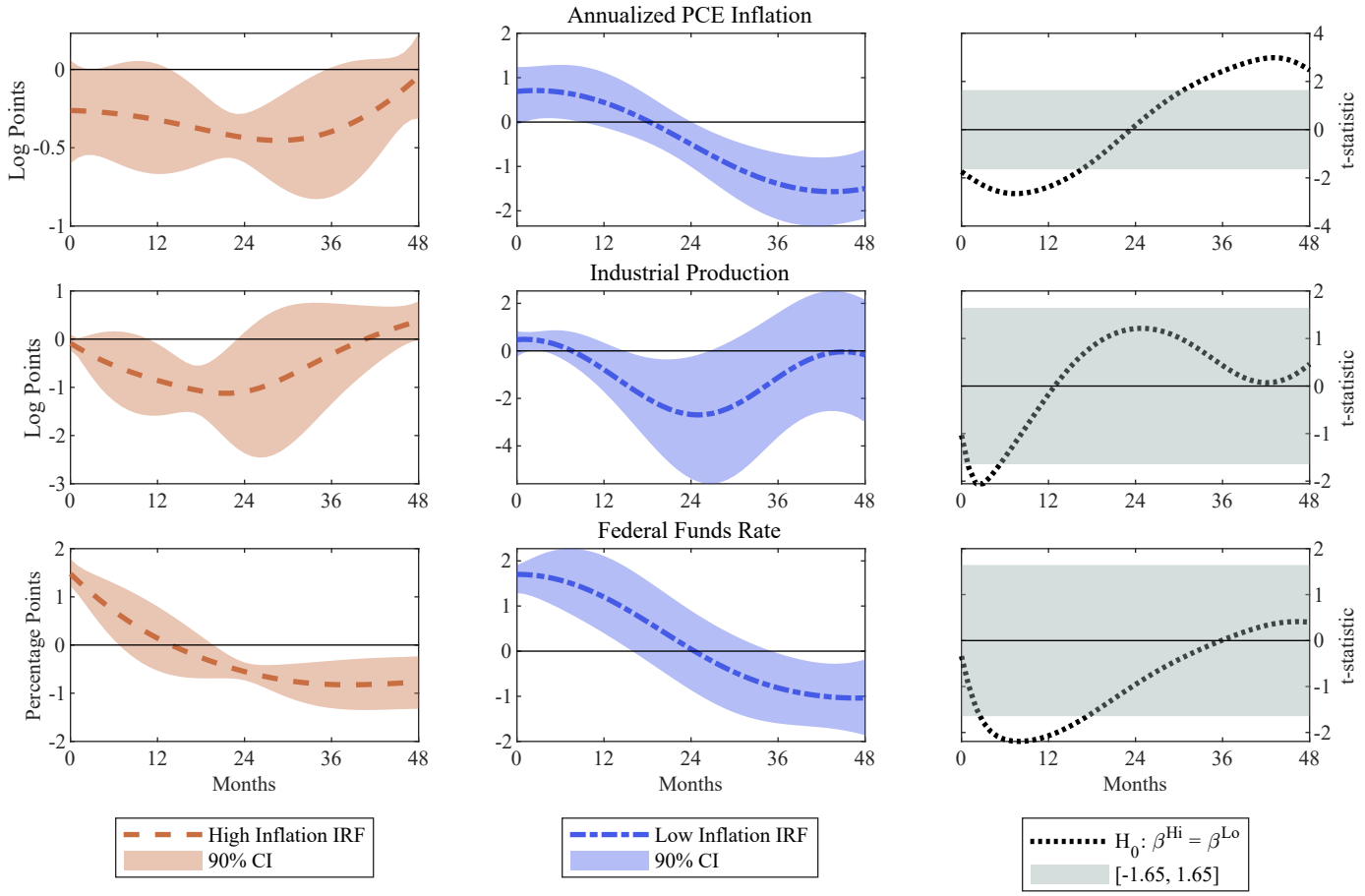

Figure H19: Panel of smooth impulse response functions in different inflation states, using non-linearly identified Romer and Romer shocks. The three response variables are annualized PCE Inflation (first row), industrial output (second row) and the federal funds rate (third row). The first column depicts the point estimates of the high inflation impulse response (dashed line) together with its 90% confidence interval. The second column depicts the point estimates of the low inflation impulse response (dashed-dotted line) together with its 90% confidence interval. The third column depicts the t-statistic for the null hypothesis of equality of the high and low inflation impulse responses (dotted line), together with the 90% z-values (grey area). All of the coefficients are depicted over a four year horizon.

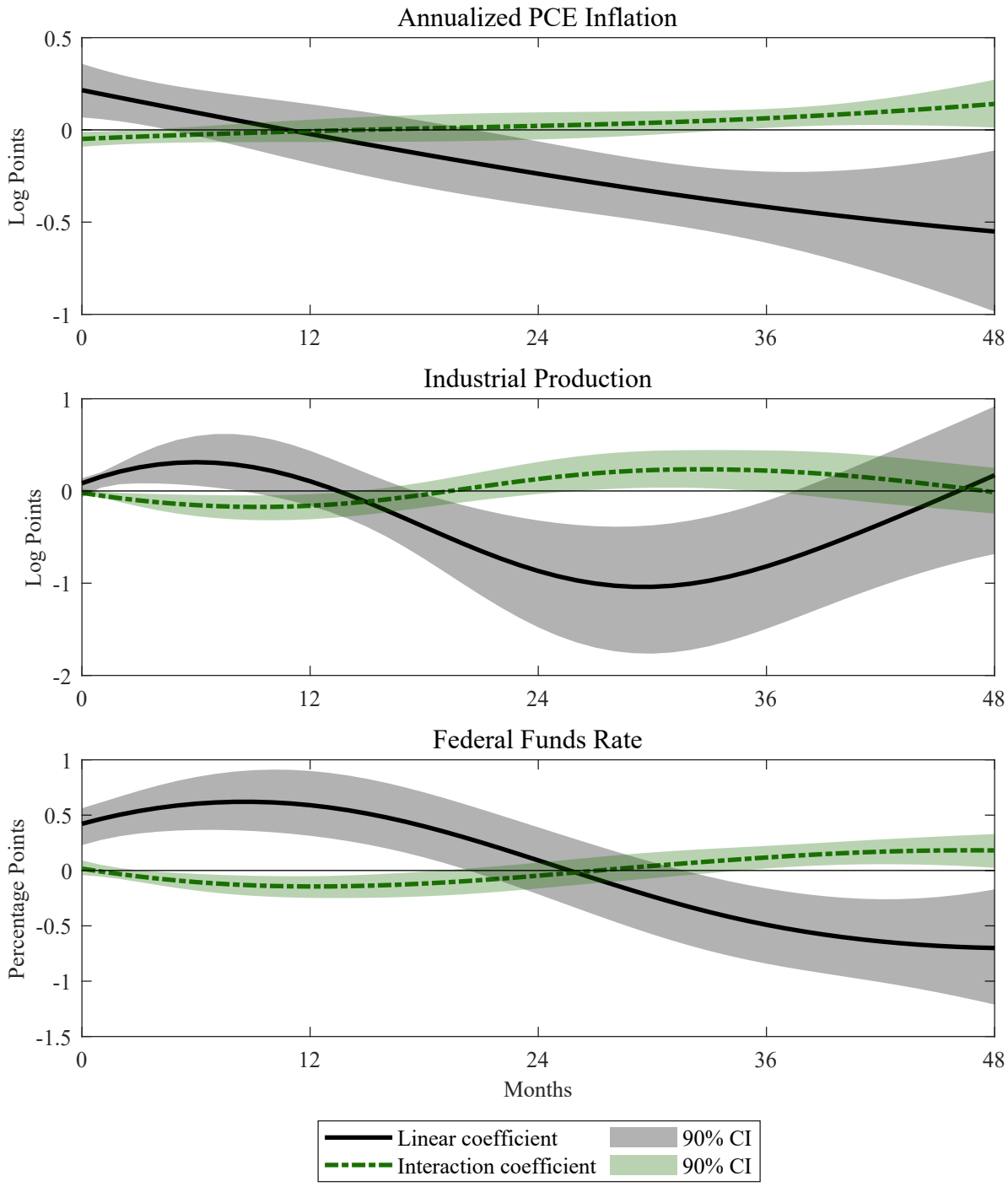

Figure H20: Panel of smooth local projection coefficients, using shocks identified from a Smooth Transition VAR. The three response variables are annualized PCE Inflation, industrial output and the federal funds rate. Every row depicts both the point estimates of the linear coefficient (solid line) and the absolute value interaction coefficient (dashed-dotted), together with their 90% confidence intervals for the various response variables. All of the coefficients are depicted over a four year horizon.

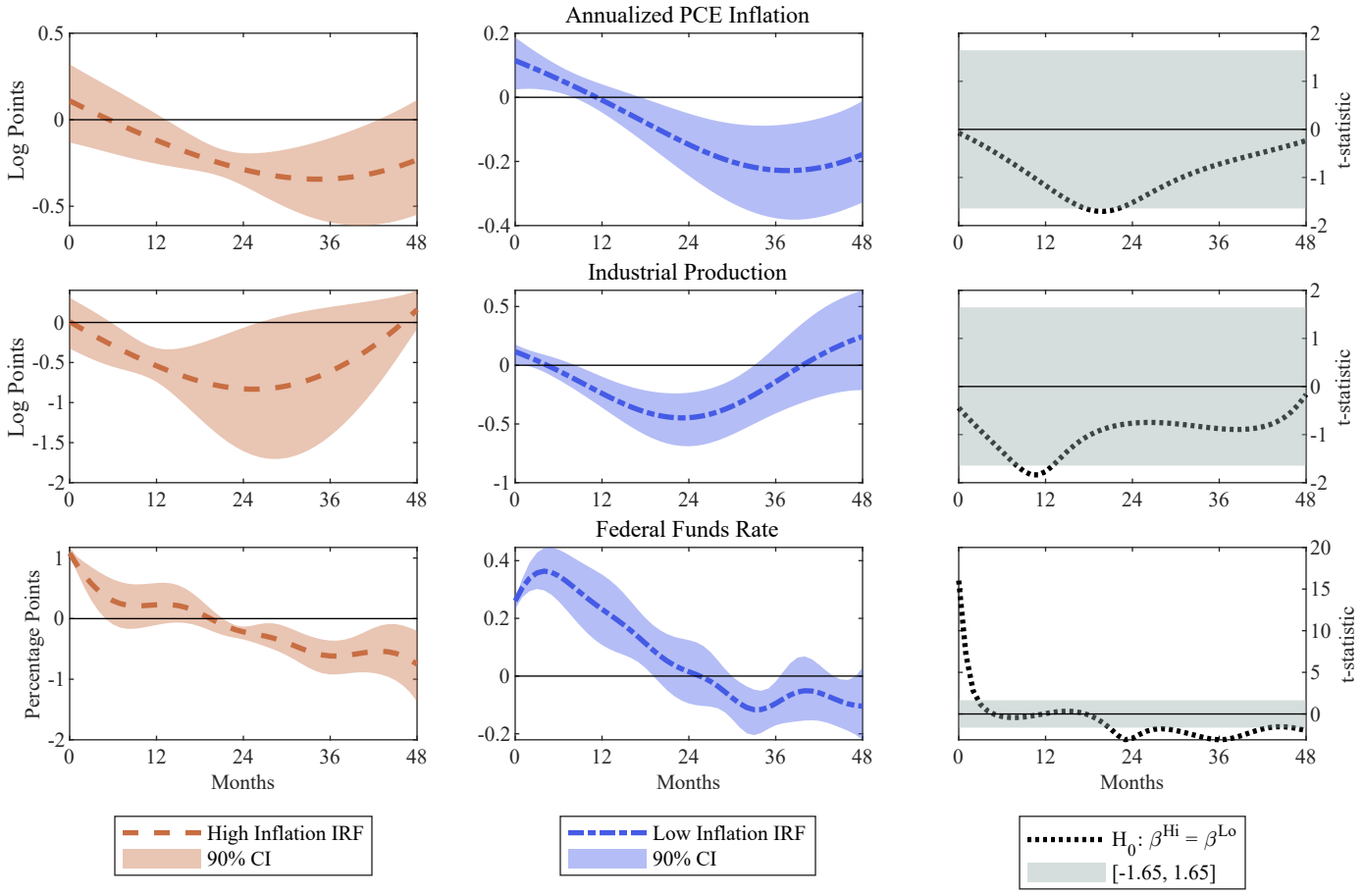

Figure H21: Panel of smooth impulse response functions in different inflation states, using shocks identified from a Smooth Transition VAR. The three response variables are annualized PCE Inflation (first row), industrial output (second row) and the federal funds rate (third row). The first column depicts the point estimates of the high inflation impulse response (dashed line) together with its 90% confidence interval. The second column depicts the point estimates of the low inflation impulse response (dashed-dotted line) together with its 90% confidence interval. The third column depicts the t-statistic for the null hypothesis of equality of the high and low inflation impulse responses (dotted line), together with the 90% z-values (grey area). All of the coefficients are depicted over a four year horizon.

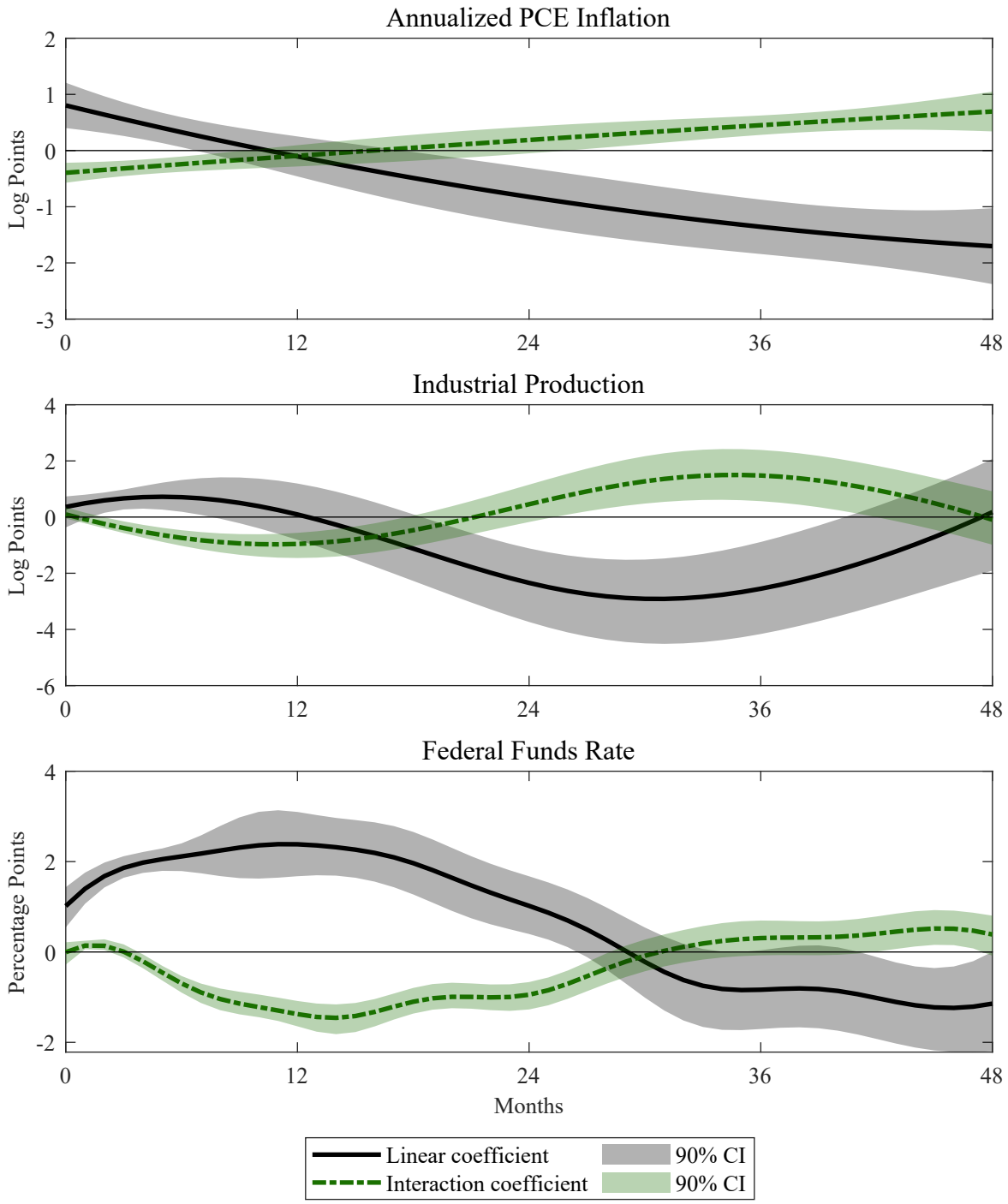

Figure H22: Panel of smooth local projection coefficients, controlling for one lead and one lag of the shock itself. The three response variables are annualized PCE Inflation, industrial output and the federal funds rate. Every row depicts both the point estimates of the linear coefficient (solid line) and the absolute value interaction coefficient (dashed-dotted), together with their 90% confidence intervals for the various response variables. All of the coefficients are depicted over a four year horizon.

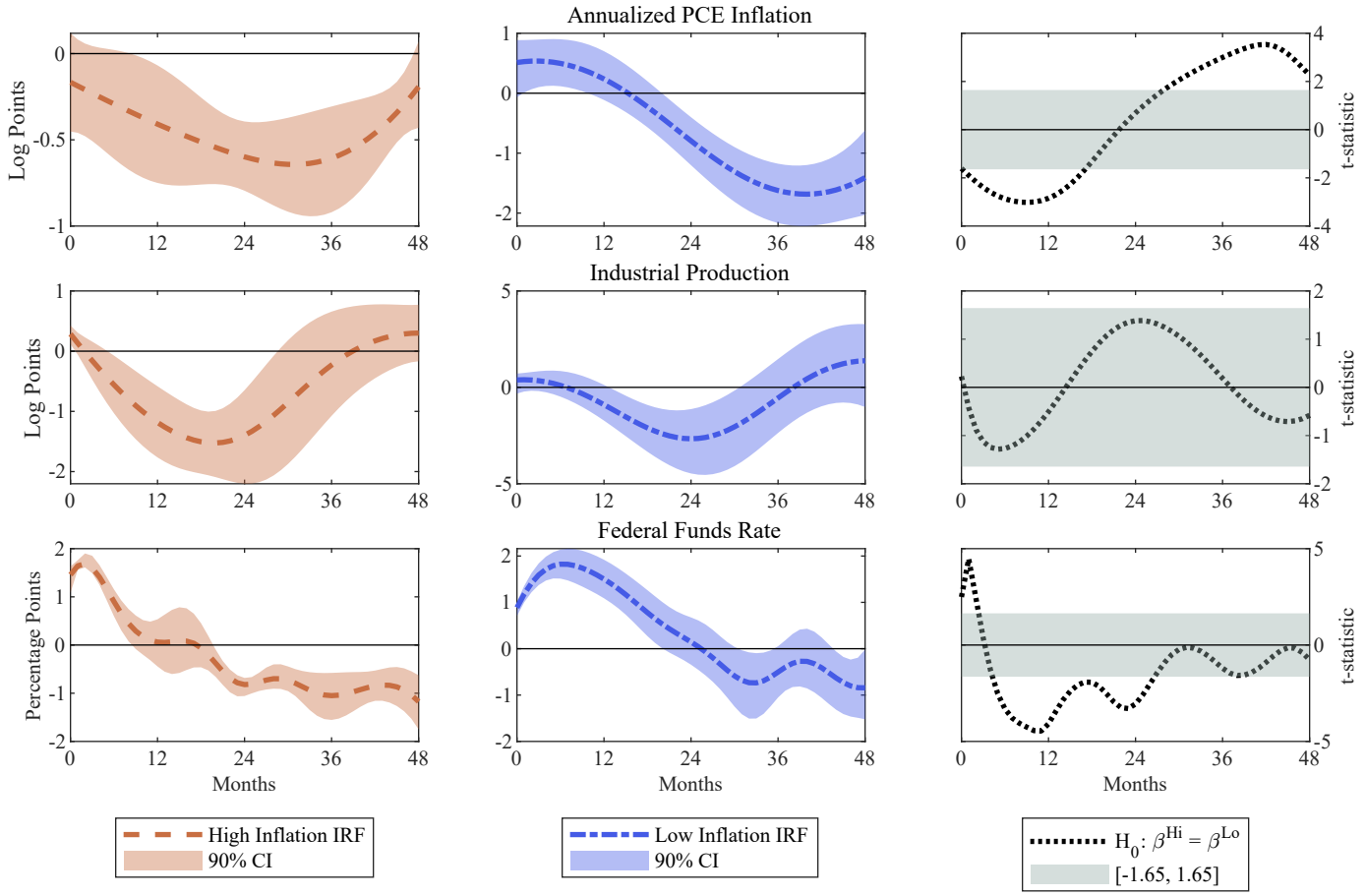

Figure H23: Panel of smooth impulse response functions in different inflation states, controlling for for one lead and one lag of the shock itself. The three response variables are annualized PCE Inflation (first row), industrial output (second row) and the federal funds rate (third row). The first column depicts the point estimates of the high inflation impulse response (dashed line) together with its 90% confidence interval. The second column depicts the point estimates of the low inflation impulse response (dashed-dotted line) together with its 90% confidence interval. The third column depicts the t-statistic for the null hypothesis of equality of the high and low inflation impulse responses (dotted line), together with the 90% z-values (grey area). All of the coefficients are depicted over a four year horizon.

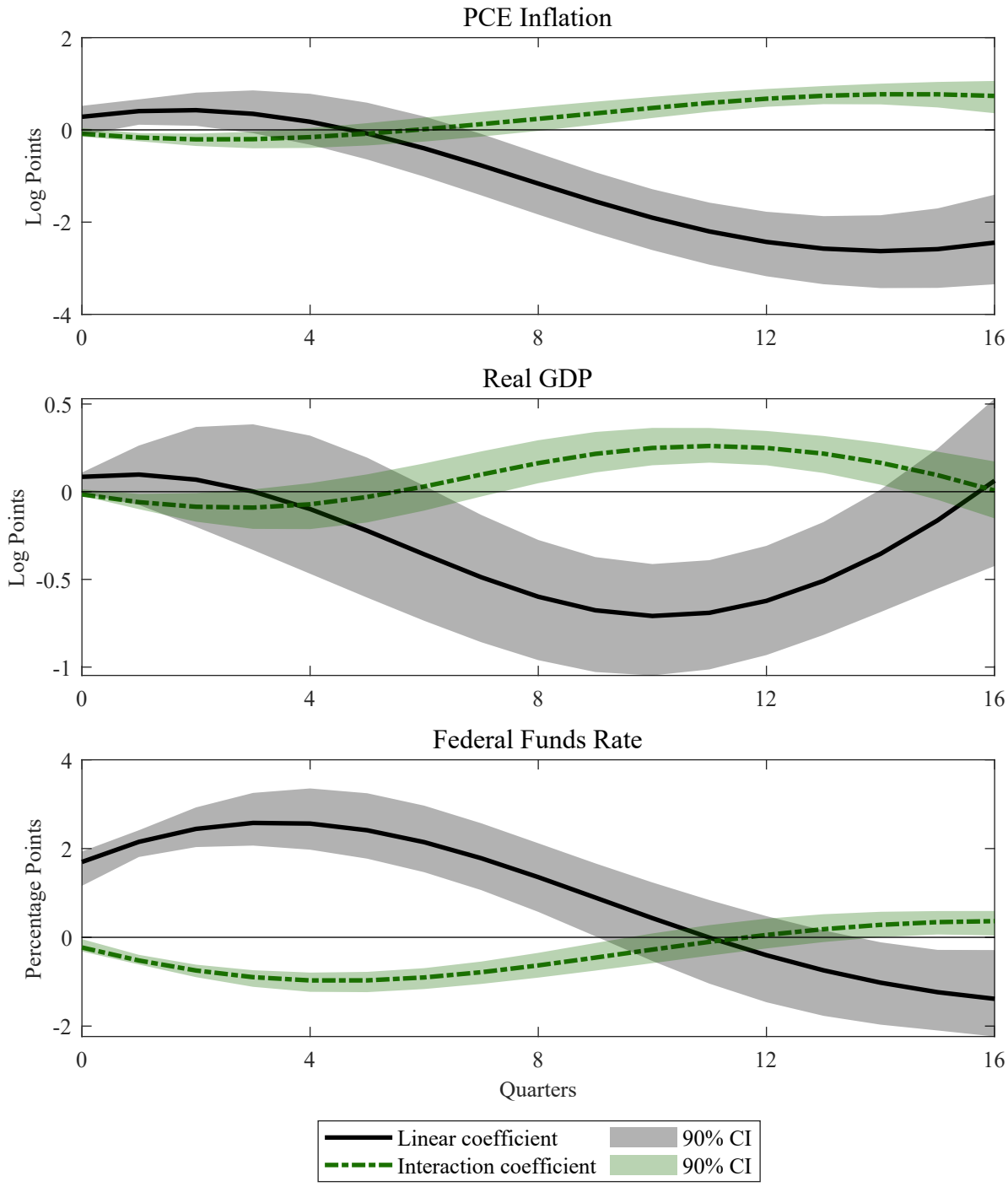

Figure H24: Panel of smooth local projection coefficients, quarterly estimation, using real GDP as the output measure. The three response variables are annualized PCE Inflation, real GDP and the federal funds rate. Every row depicts both the point estimates of the linear coefficient (solid line) and the absolute value interaction coefficient (dashed-dotted), together with their 90% confidence intervals for the various response variables. All of the coefficients are depicted over a four year horizon.

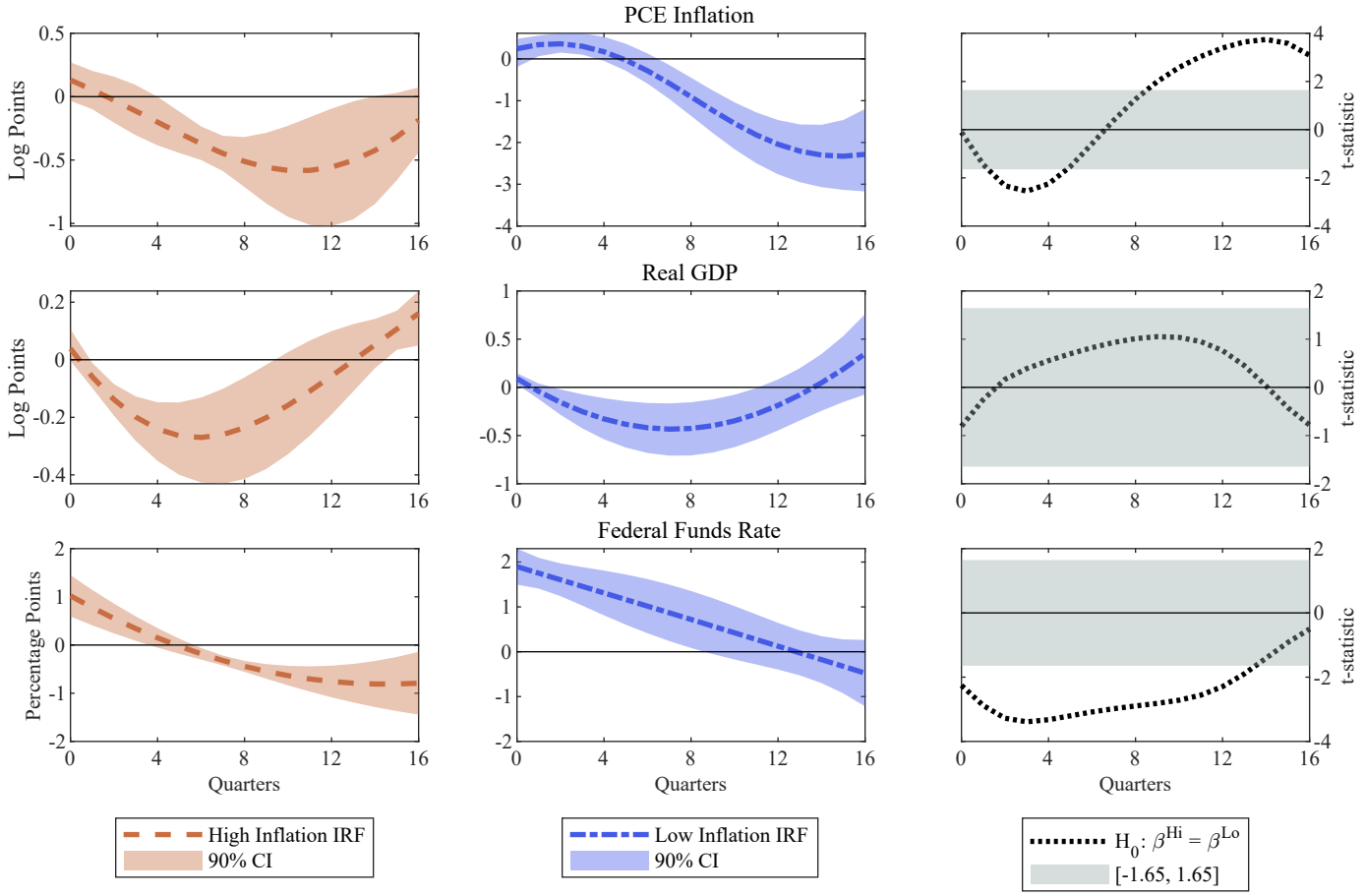

Figure H25: Panel of smooth impulse response functions in different inflation states, quarterly estimation, using real GDP as the output measure. The three response variables are annualized PCE Inflation (first row), real GDP (second row) and the federal funds rate (third row). The first column depicts the point estimates of the high inflation impulse response (dashed line) together with its 90% confidence interval. The second column depicts the point estimates of the low inflation impulse response (dashed-dotted line) together with its 90% confidence interval. The third column depicts the t-statistic for the null hypothesis of equality of the high and low inflation impulse responses (dotted line), together with the 90% z-values (grey area). All of the coefficients are depicted over a four year horizon.

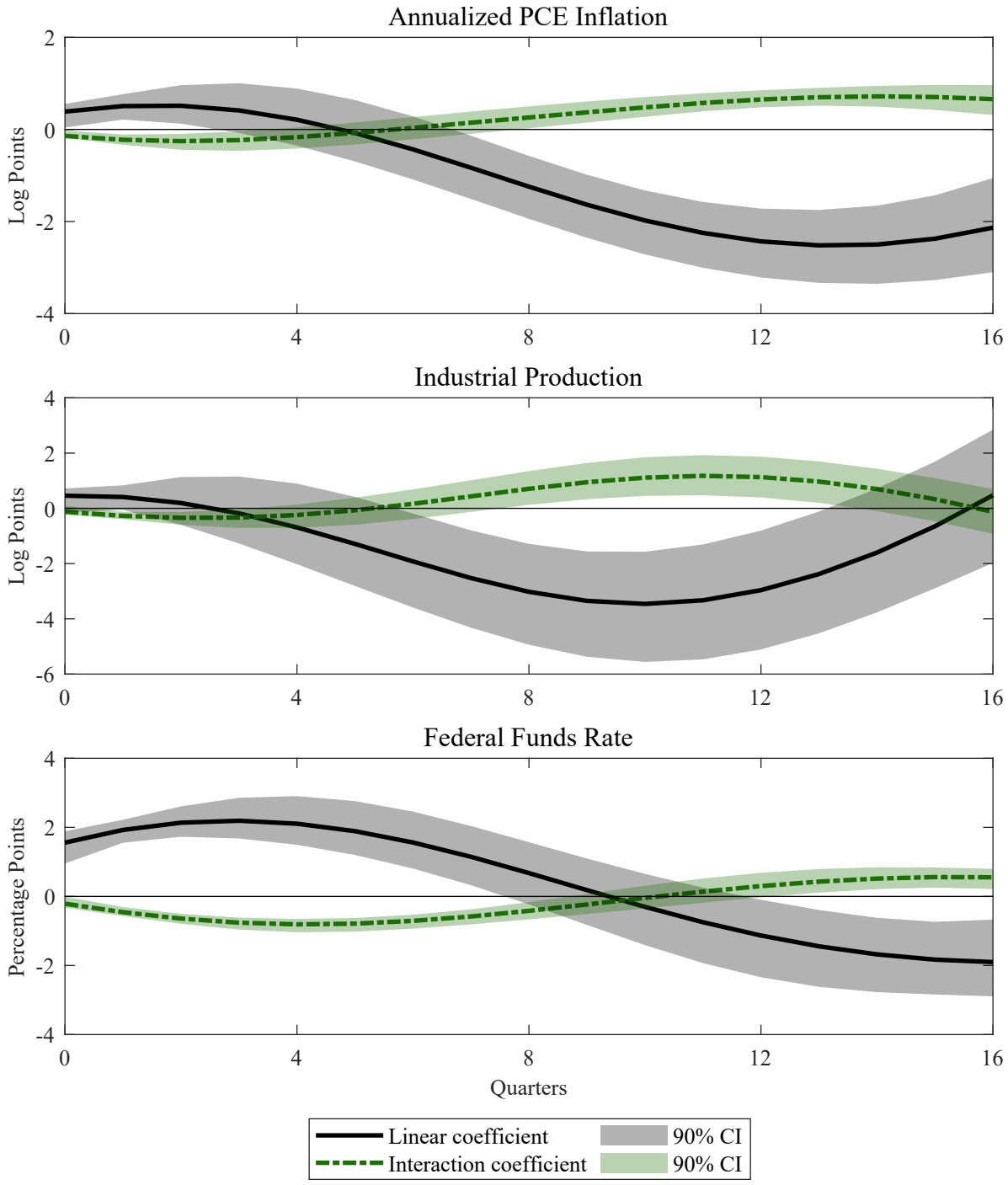

Figure H26: Panel of smooth local projection coefficients, quarterly estimation, controlling for fiscal policy with the Fisher and Peters (2010) shocks. The three response variables are annualized PCE Inflation, industrial output and the federal funds rate. Every row depicts both the point estimates of the linear coefficient (solid line) and the absolute value interaction coefficient (dashed-dotted), together with their 90% confidence intervals for the various response variables. All of the coefficients are depicted over a four year horizon.

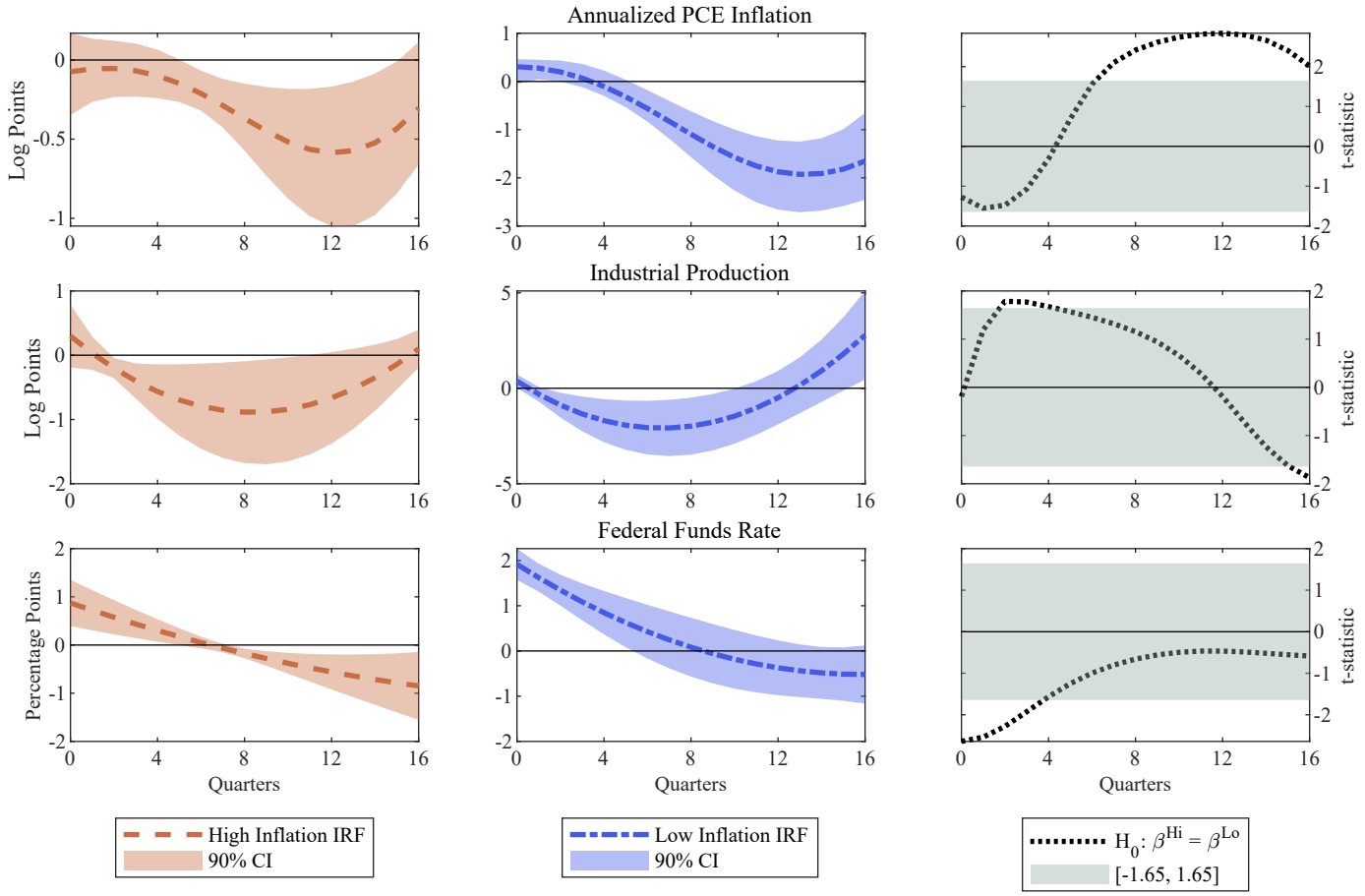

Figure H27: Panel of smooth impulse response functions in different inflation states, quarterly estimation, controlling for fiscal policy with the Fisher and Peters (2010) shocks. The three response variables are annualized PCE Inflation (first row), industrial output (second row) and the federal funds rate (third row). The first column depicts the point estimates of the high inflation impulse response (dashed line) together with its 90% confidence interval. The second column depicts the point estimates of the low inflation impulse response (dashed-dotted line) together with its 90% confidence interval. The third column depicts the t-statistic for the null hypothesis of equality of the high and low inflation impulse responses (dotted line), together with the 90% z-values (grey area). All of the coefficients are depicted over a four year horizon.

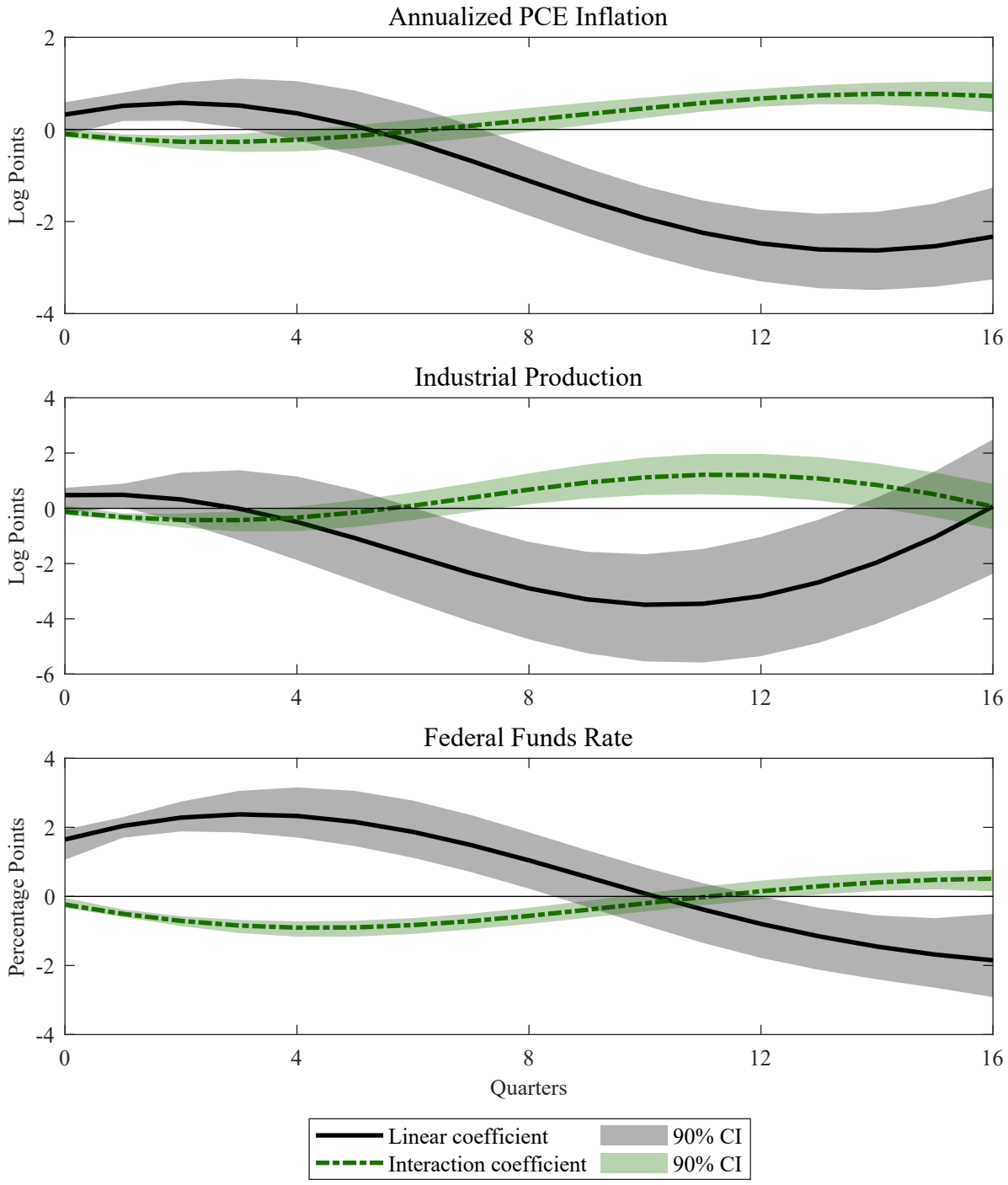

Figure H28: Panel of smooth local projection coefficients, quarterly estimation, fiscal policy with the Romer and Romer (2010) exogenous tax series. The three response variables are annualized PCE Inflation, industrial output and the federal funds rate. Every row depicts both the point estimates of the linear coefficient (solid line) and the absolute value interaction coefficient (dashed-dotted), together with their 90% confidence intervals for the various response variables. All of the coefficients are depicted over a four year horizon.

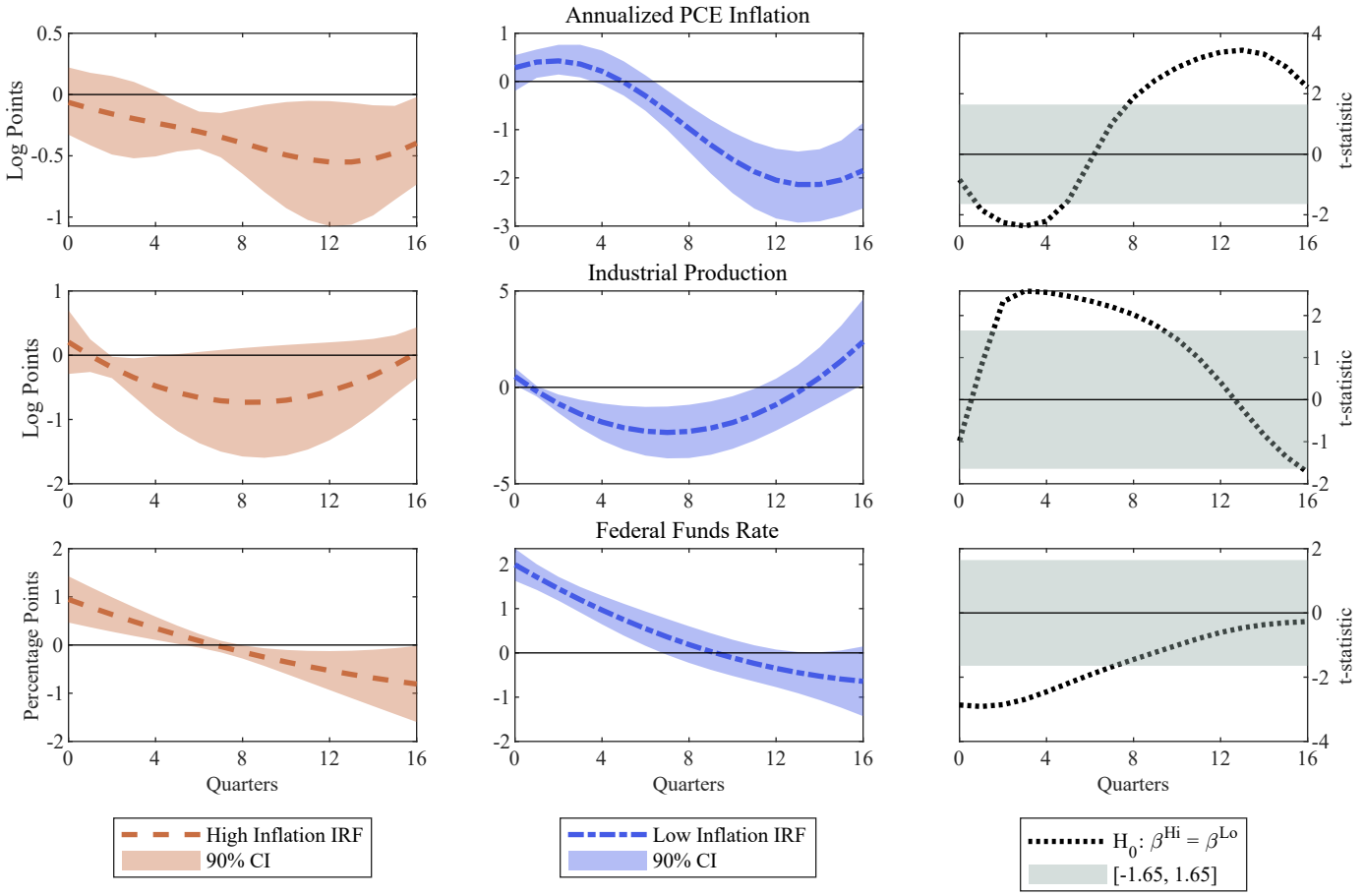

Figure H29: Panel of smooth impulse response functions in different inflation states, quarterly estimation, controlling for fiscal policy with the Romer and Romer (2010) exogenous tax series. The three response variables are annualized PCE Inflation (first row), industrial output (second row) and the federal funds rate (third row). The first column depicts the point estimates of the high inflation impulse response (dashed line) together with its 90% confidence interval. The second column depicts the point estimates of the low inflation impulse response (dashed-dotted line) together with its 90% confidence interval. The third column depicts the t-statistic for the null hypothesis of equality of the high and low inflation impulse responses (dotted line), together with the 90% z-values (grey area). All of the coefficients are depicted over a four year horizon.

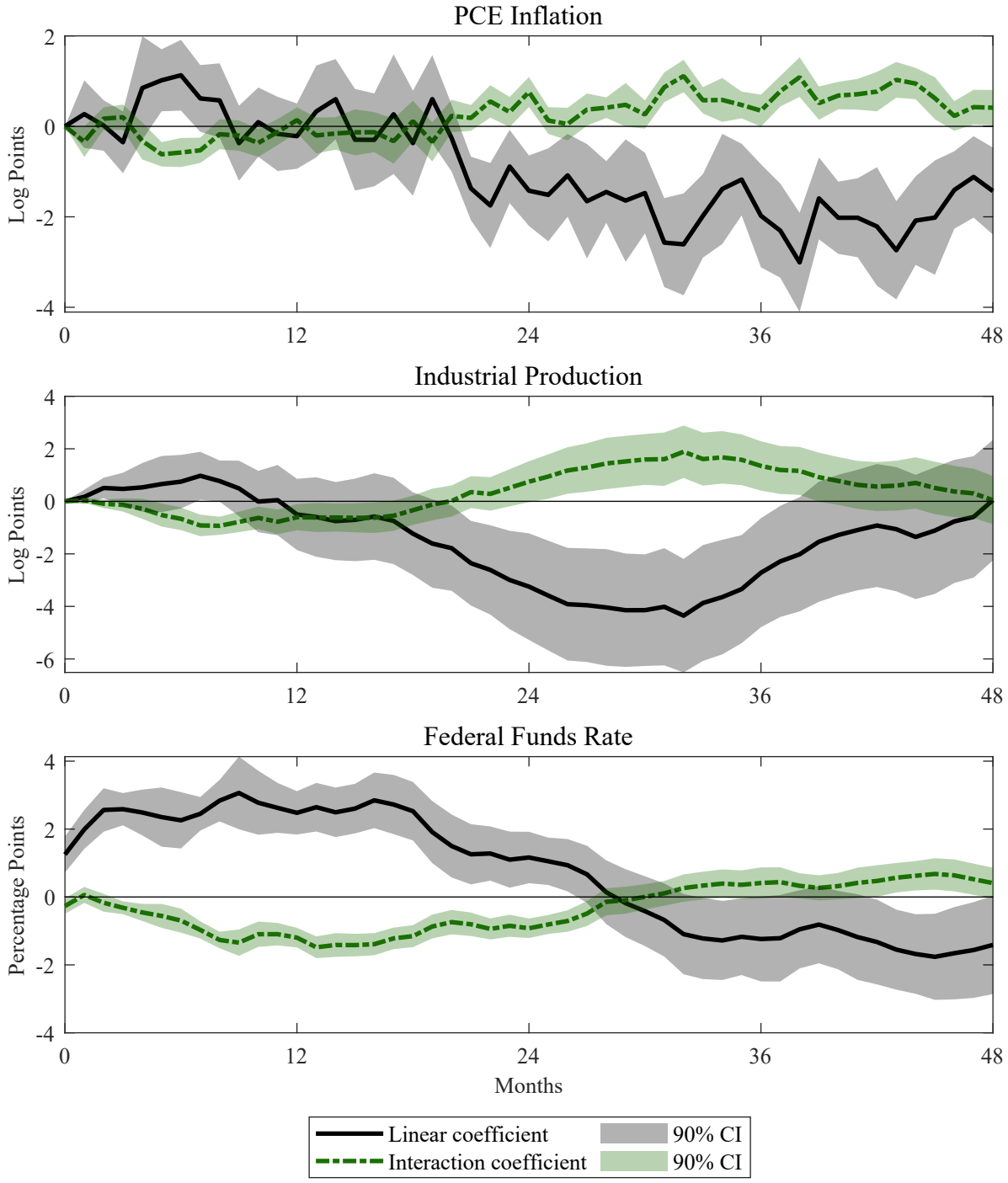

Figure H30: Panel of local projection coefficients, unsmoothed. The three response variables are annualized PCE Inflation, industrial output and the federal funds rate. Every row depicts both the point estimates of the linear coefficient (solid line) and the absolute value interaction coefficient (dashed-dotted), together with their 90% confidence intervals for the various response variables. All of the coefficients are depicted over a four year horizon.

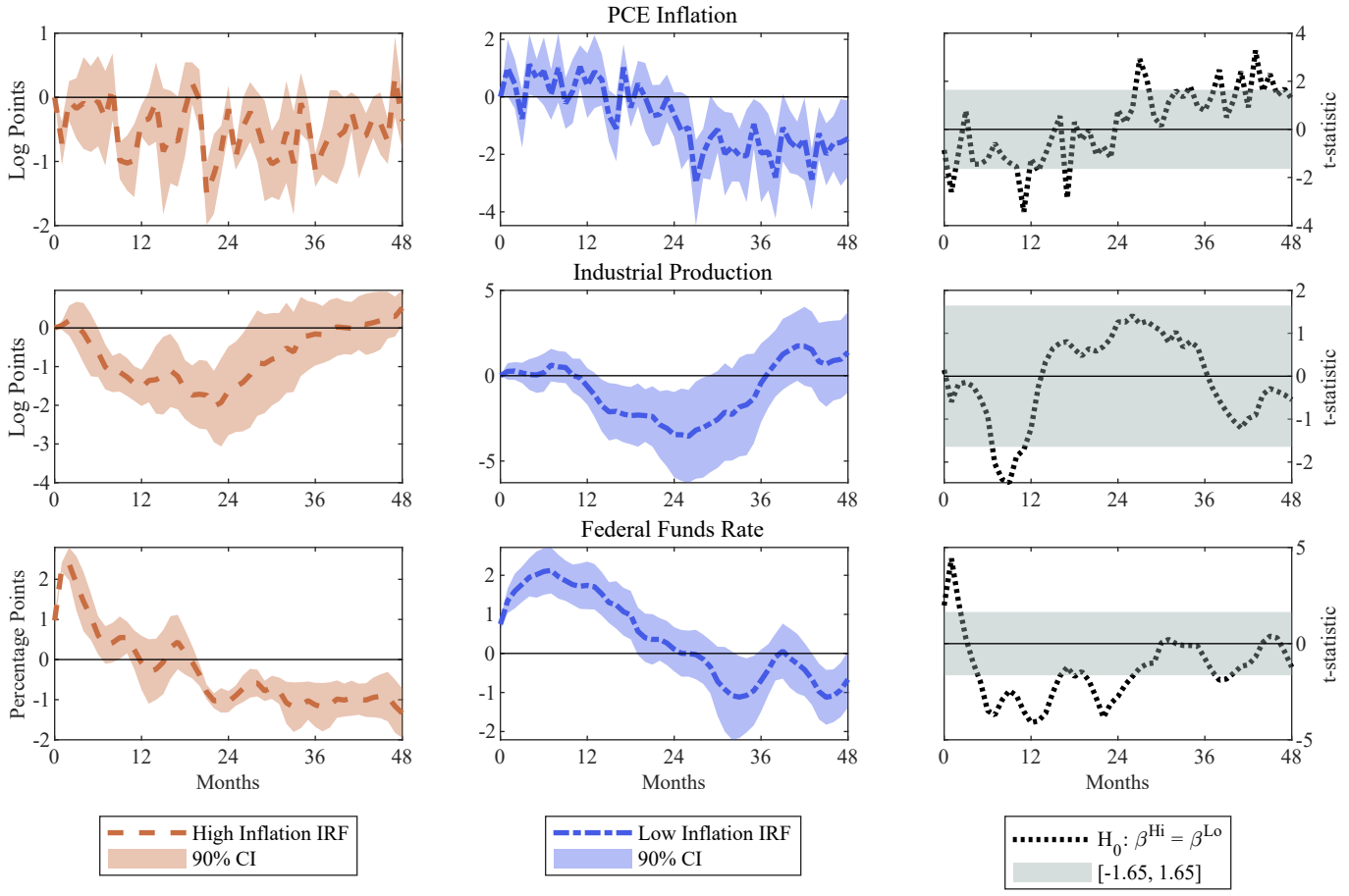

Figure H31: Panel of impulse response functions in different inflation states, unsmoothed. The three response variables are annualized PCE Inflation (first row), industrial output (second row) and the federal funds rate (third row). The first column depicts the point estimates of the high inflation impulse response (dashed line) together with its 90% confidence interval. The second column depicts the point estimates of the low inflation impulse response (dashed-dotted line) together with its 90% confidence interval. The third column depicts the t-statistic for the null hypothesis of equality of the high and low inflation impulse responses (dotted line), together with the 90% z-values (grey area). All of the coefficients are depicted over a four year horizon.

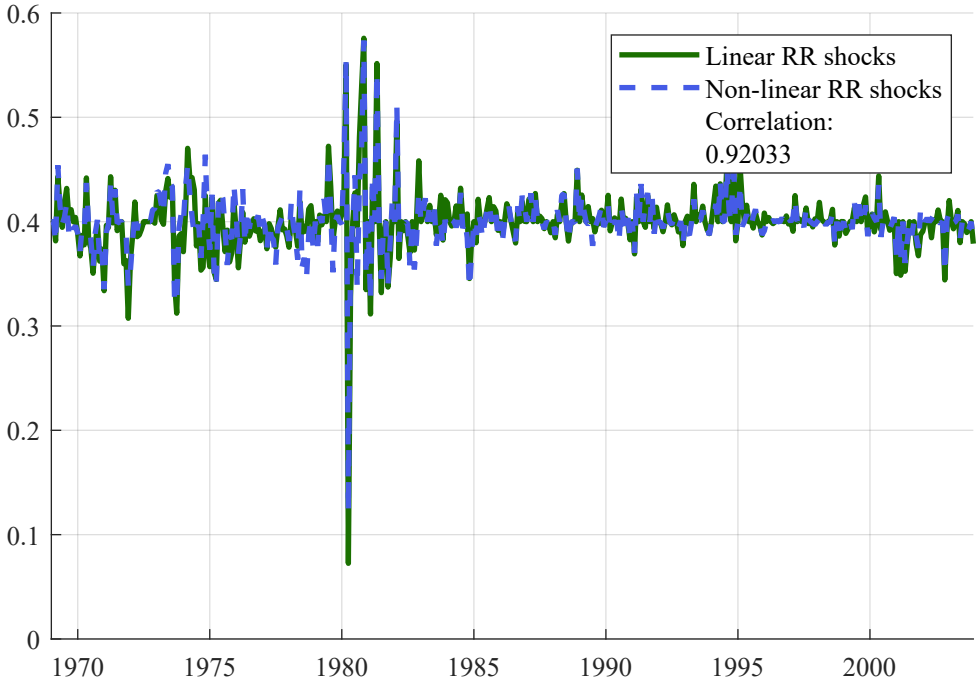

Figure H32: Time series of linear and non-linear Romer and Romer shocks used in this study. The linear shocks are indicated by the solid line, whereas the non-linear shocks are indicated by the dashed line. The correlation coefficient between two shock series is equal to 0.92, as indicated in the top right hand corner.

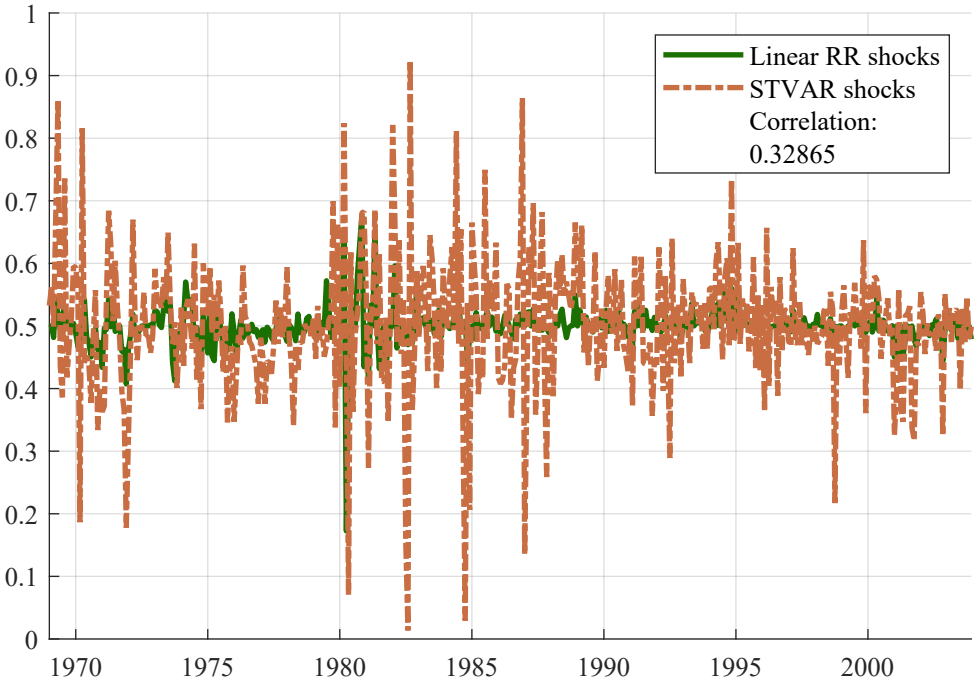

Figure H33: Time series of linear Romer and Romer and STVAR shocks used in this study. The linear shocks are indicated by the solid line, whereas the STVAR shocks are indicated by the dashed-dotted line. The correlation coefficient between the two shock series is equal to 0.32, as indicated in the top right hand corner.

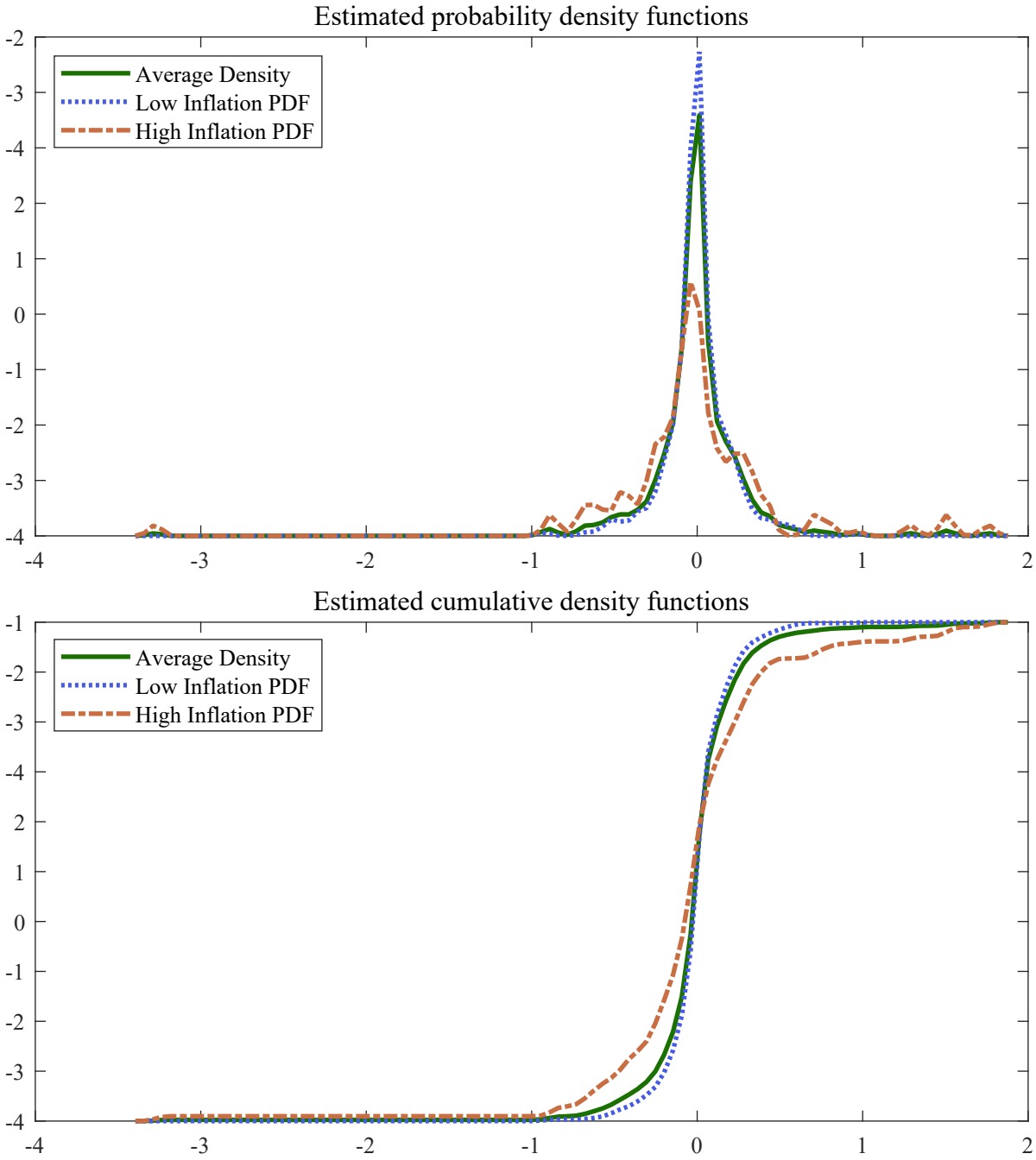

Figure H34: Distribution of shocks over high and low trend inflation regimes: Panel A shows the estimated probability density functions whilst Panel B shows the estimated cumulative density function. The average density is indicated by the solid line, the low inflation density with the dotted line and the high inflation density with the dashed-dotted line.

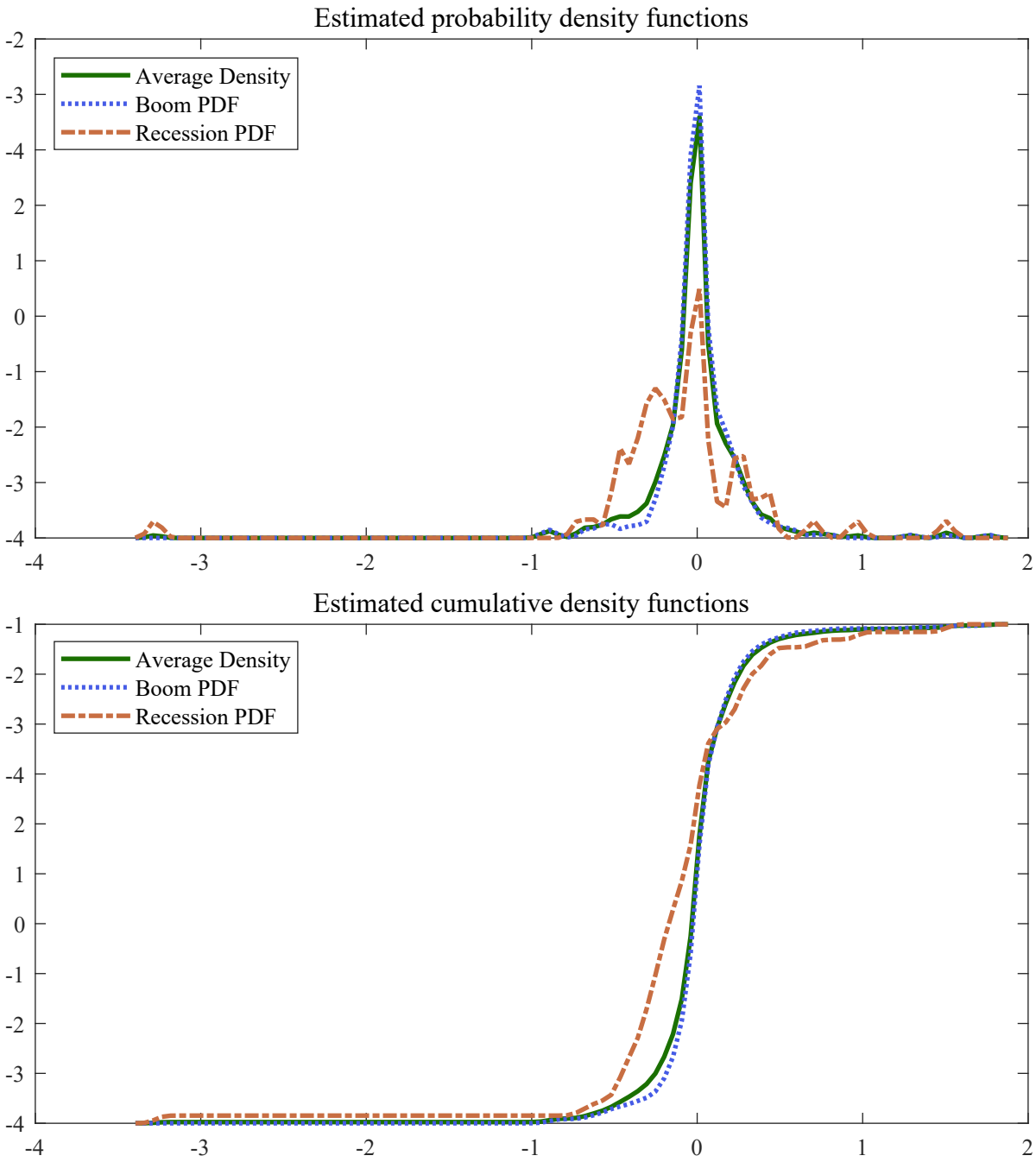

Figure H35: Distribution of shocks over booms and recessions: Panel A shows the estimated probability density functions whilst Panel B shows the estimated cumulative density functions. The average density is indicated by the solid line, the expansion density with the dotted line and the recession density with the dashed-dotted line.

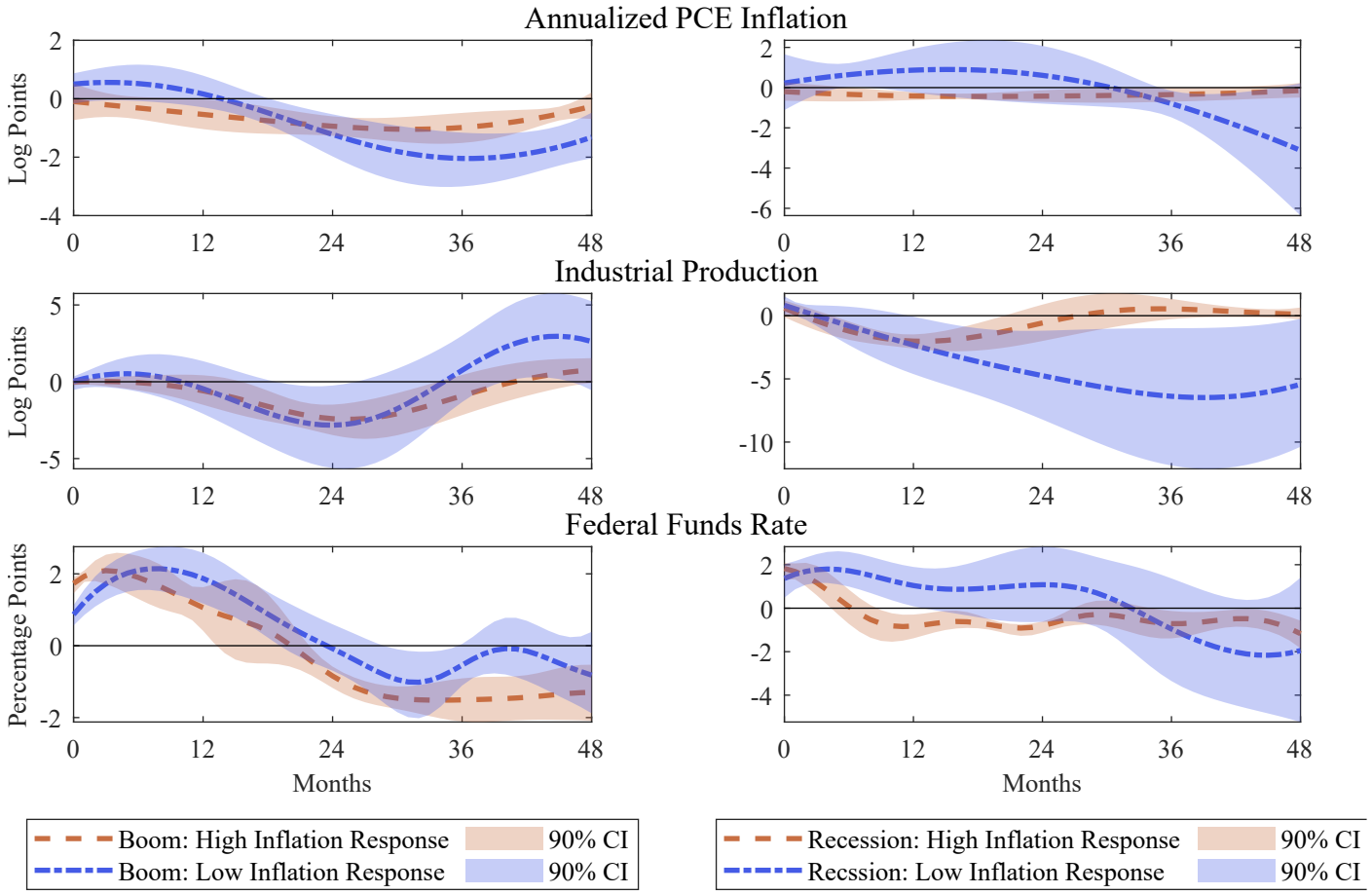

Figure H36: Panel of smooth impulse response functions in different inflation states and in different business cycles states, ie. recessions and expansions, as defined by the NBER recession dates. The three response variables are annualized PCE Inflation (first row), industrial output (second row) and the federal funds rate (third row). The first column depicts the point estimates of the high (dashed line) and low (dashed-dotted line) inflation impulse response together with its 90% confidence interval in economic expansions. The second column depicts the point estimates of the high (dashed line) and low (dashed-dotted line) inflation impulse response together with its 90% confidence interval in economic recessions. All of the coefficients are depicted over a four year horizon.

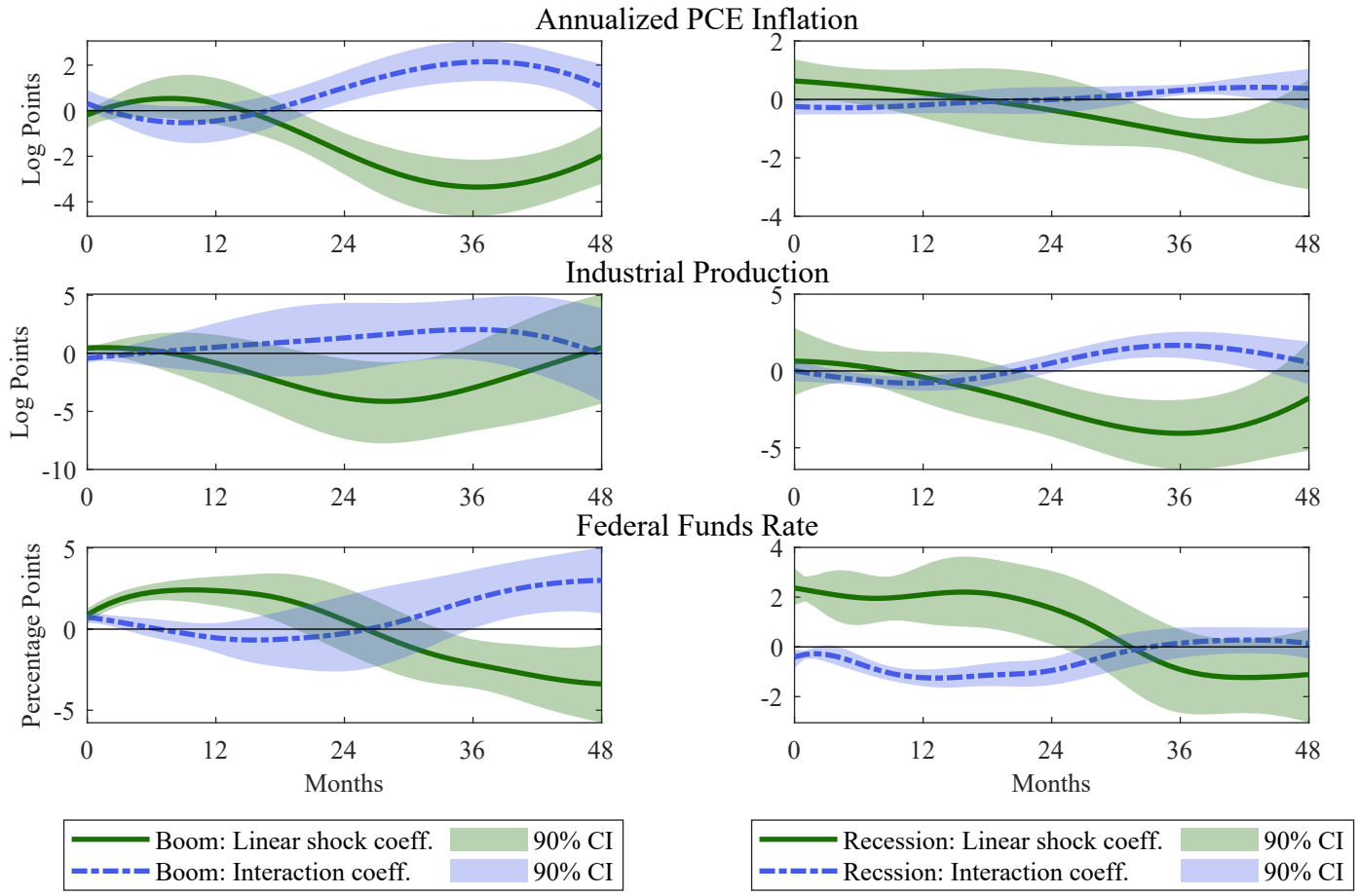

Figure H37: Panel of smooth local projection coefficients, in both expansions and recessions, as defined by the NBER recession dates. The three response variables are annualized PCE Inflation, industrial output and the federal funds rate. The first column depicts both the point estimates of the linear coefficient (solid line) and the absolute value interaction coefficient (dashed-dotted), together with their 90% confidence intervals in economic expansions. The second column depicts both the point estimates of the linear coefficient (solid line) and the absolute value interaction coefficient (dashed-dotted), together with their 90% confidence intervals in economic recessions. All of the coefficients are depicted over a four year horizon.

I Tables

Δ IP Local Projection - Hansen (1992) test statistic

Horizon	$h = 1$	$h = 3$	$h = 6$	$h = 12$	$h = 24$	$h = 36$
Linear coefficient	0.11	0.09	0.17	0.14	0.22	0.20
Interaction coefficient	0.02	0.03	0.01	0.03	0.05	0.19
Joint: all coefficients	3.02^{**}	4.04^{***}	4.38^{***}	4.26^{***}	3.64^{***}	3.68^{***}

Table I1: Estimated Hansen (1992) test statistics for parameter constancy of the change of industrial production local projection with both a linear and an absolute value interaction shock term. The first row reports the individual test statistic for the linear coefficient at different horizons, the second row reports those for the absolute value interaction coefficient and the final row reports the test statistic for the joint hypothesis of all parameters (ie. regression coefficients and variance) to be constant.
Individual critical values are $c_{1,1\%} = 0.75$, $c_{1,5\%} = 0.47$ *and* $c_{1,10\%} = 0.35$. *Joint critical values for a model with* $K = 12$ *parameters are* $c_{12,1\%} = 3.51$, $c_{12,5\%} = 2.96$ *and* $c_{12,10\%} = 2.69$.
****: Significant at the 1% level; **: Significant at the 5% level; *: Significant at the 10% level;*

Δ FFR Local Projection - Hansen (1992) test statistic

Horizon	$h = 1$	$h = 3$	$h = 6$	$h = 12$	$h = 24$	$h = 36$
Linear coefficient	0.13	0.05	0.03	0.11	0.11	0.18
Interaction coefficient	0.02	0.01	0.01	0.03	0.05	0.14
Joint: all coefficients	3.36**	2.28	2.45	4.19***	3.66***	2.78*

Table I2: Estimated Hansen (1992) test statistics for parameter constancy of the change of the federal funds rate local projection with both a linear and an absolute value interaction shock term. The first row reports the individual test statistic for the linear coefficient at different horizons, the second row reports those for the absolute value interaction coefficient and the final row reports the test statistic for the joint hypothesis of all parameters (ie. regression coefficients and variance) to be constant.
Individual critical values are $c_{1,1\%} = 0.75$, $c_{1,5\%} = 0.47$ and $c_{1,10\%} = 0.35$. Joint critical values for a model with $K = 12$ parameters are $c_{12,1\%} = 3.51$, $c_{12,5\%} = 2.96$ and $c_{12,10\%} = 2.69$.
****: Significant at the 1% level; **: Significant at the 5% level; *: Significant at the 10% level*

Shock summary statistics

Statistic	Linear R&R Shock	Non-linear R&R Shock	STVAR Shock
Mean	-0.004	-0.002	0.006
Median	0	0	0.029
Std. dev.	0.312	0.288	1.073
Min.	-3.275	-2.776	-4.863
Max.	1.758	1.735	4.246
AR(1) Coefficient	0.084	0.009	-0.034

Table I3: Summary statistics for the monetary policy shocks used in the analysis